Tsunami frequency analysis for Eastern Coromandel and Waikato Region from Kermadec Trench and local sources within the Bay of Plenty

G. Prasetya X. Wang

GNS Science Consultancy Report 2011/135
June 2011

DISCLAIMER

BIBLIOGRAPHIC REFERENCE

Prasetya, G. and Wang, X. 2011. Tsunami frequency analysis for Eastern Coromandel and Waikato Region from Kermadec Trench and local sources within the Bay of Plenty, *GNS Science Consultancy Report* 2011/135. 65 p.

CONTENTS

FIGURES

TABLES

APPENDICES

EXECUTIVE SUMMARY

1. Environment Waikato (EW) provided research funding for GNS Science to undertake an analysis of tsunami frequency for tsunami events sourced from the Tonga-Kermadec region and local earthquake sources within the Bay of Plenty for the Eastern Coromandel Peninsula and east coast of Waikato Region through:

   - An overview of the previous and recent tsunami hazards research relevant to the Eastern Coromandel Peninsula through all relevant publications related to tsunami hazard assessment for Eastern Coromandel Peninsula, clustering tsunami source definitions for the region from the Tonga-Kermadec source area, and a review of numerical modelling approaches applied to tsunami generation, propagation and inundation that had been used with source of bathymetry and topography data;

   - A description of the uncertainties associated with the Tonga-Kermadec source region in generating tsunami through a discussion of the seismicity and slip partitioning of large shallow earthquakes, paleo-tsunami deposits, and the role of sediment thickness on the subduction zone and related seismicity and tsunami genesis;

   - Estimated potential return periods for tsunami generated from the Tonga-Kermadec region through a review of Tonga-Kermadec Trench seismicity based on published data and reports, the application of McCaffrey (2008) methods to determine possible maximum earthquakes from the Tonga-Kermadec Trench, and computation of potential tsunami heights based on the methods of Abe (1995).

   - Regional Numerical modelling for Coromandel and Waikato Region from potential sources along the Kermadec Trench and local sources within Bay of Plenty Region.

2. Study results show:

   - A consistent result on the potential tsunami impact to the region. These regions are highly susceptible to a tsunami generated from the Kermadec Trench. All studies show that sources that extend from the East Cape Ridge to the northeast across the Rapuhia Scarp up to the central of Kermadec Trench (central and southern segment) provide a significant impact to the eastern Coromandel and along the east coast of Waikato region. The regional numerical modelling assessment for individual segment ruptures shows the southern and central segments (Mw 8.5 to 8.9) provide a significant impact to the region with maximum tsunami elevation at the coast ranges from 3 to 5 m. The numerical modelling assessment shows that the maximum tsunami elevation based on the entire rupture of Kermadec Trench scenario and the possible extent to the Hikurangi Margin (Mw > 9.0) ranges from 8 m to 15 m above MSL, and 12 to 18 m (peak to trough) using an empirical formula of Abe (1995). Detailed inundation modelling is needed to quantify the extent of inundation and the local effects that contribute in amplifying or reducing the tsunami height.

   - The uncertainty assessments associated with the Tonga-Kermadec source region in generating a tsunami show that the event scenario involving the entire rupture of the Kermadec Trench (segment A, B and C of Power et al.2011; segments 2, 3 and 4 of this study; or southern, central and northern segment of previous studies of Goff et al. 2006, De Lange et al. 2008) in the logic tree is unlikely to occur as only 12%

weighting was assigned to a magnitude frequency distribution that permit ruptures as large as Mw 9.4 to occur (Power et al. 2011). However, this scenario is taken into account (Power et al. 2011) as the possibility of rupture of the entire trench cannot be ruled out empirically (McCaffrey, 2007). The Sumatra earthquake – Indian Ocean Tsunamis - ruptured more than 1250 km of fault ruptures resulting in a magnitude ~ Mw = 9.2. This event occurred in a region that was thought incapable of generating such a large earthquake (McCaffrey, 2008). Furthermore, a recent paleo-tsunami study along the North Island New Zealand (Goff et al. 2010) presents evidence for tsunami deposit in ~AD1450's along the North Island that can be correlated with the tsunami height distribution pattern from tsunamis generated by the scenario events that involve the rupturing the entire Kermadec Trench.

- Estimated potential return periods for tsunamis generated from the Tonga-Kermadec region show that the large events may take place at 600 to 800 years recurrence for earthquakes even greater than Mw =9.0 with maximum tsunami wave height (peak to trough) up to 18 m, and up to 8 m (peak to trough) every ~ 400 years (Mw $\leq$ 9.0).

- The numerical modelling from the local sources within the Bay of Plenty shows that the maximum tsunami impact is produced by the Astrolabe composite fault with maximum tsunami elevation above MSL along the east coast of Waikato region ranges from 0.5 to 1.5 m. This fault has a typical return period varying from few hundred to 1000's of years (Lamarche and Barnes, 2005).

1.0 INTRODUCTION

Environment Waikato (EW) provided research funding for GNS Science to undertake an analysis of tsunami frequency for tsunami events sourced from the Tonga-Kermadec region and local earthquake within the Bay of Plenty for the Eastern Coromandel Peninsula and east coast of Waikato Region. A previous study by Bell et al., (2004) acknowledged that developing an understanding of the frequency/magnitude of all local and regional source tsunami events in the vicinity of New Zealand is a long-term project that requires significant field investigations. By necessity these should include marine geology and geophysical investigations, identification and recording of paleo-tsunami deposits and their integration with the historical tsunami record, and modelling of tsunami dynamics (tsunami generation, propagation and inundation).

As outlined in contract no: RCS2009/10-239, this study aims to provide:

- An overview of previous tsunami hazards research relevant to the Eastern Coromandel Peninsula contained in all relevant publications related to tsunami hazard assessment for Eastern Coromandel Peninsula, clustering tsunami source definitions for the region from the Tonga-Kermadec source area, and a review of numerical modelling approaches applied to tsunami generation, propagation and inundation that had been used with source of bathymetry and topography data;
- A description of the uncertainties associated with the Tonga-Kermadec source region in generating tsunami through a discussion of the seismicity and slip partitioning of large shallow earthquakes, paleo-tsunami deposits, and the role of sediment thickness on the subduction zone and related seismicity and tsunami genesis;
- Estimated potential return periods for tsunamis generated from the Tonga-Kermadec region through a review of Tonga-Kermadec Trench seismicity based on published data and reports, the application of McCaffrey (2008) methods to determine possible maximum earthquakes from the Tonga-Kermadec Trench, and computation of potential tsunami heights based on the methods of Abe (1995);
- Regional Numerical modelling for Coromandel and Waikato Region from potential sources along the Kermadec Trench and local sources within Bay of Plenty Region.

2.0 OVERVIEW OF PREVIOUS STUDIES

New Zealand is subject to a wide range of potential tsunami sources as a result of its position straddling the Pacific-Australian tectonic plate boundary. Two significant tsunami hazard studies have been carried out for the east, north and western seaboard of the North Island. These include the assessment of tsunami hazard and associated risk (Goff J., 2003, and Bell et al.2004), and tsunami sources for the combined councils (Northland, Auckland, Waikato and Bay of Plenty) by Goff et al. (2006). These projects were commissioned under the Joint Tsunami Research

Project commissioned by Environment Bay of Plenty (EBOP) and Environment of Waikato (EW).

2.1 Joint Tsunami Research Project of EBOP and EW (Bell et al. 2004)

Bell et al. (2004) undertook a tsunami hazard research project for the Bay of Plenty and Eastern Coromandel Peninsula. The project involved combining data and information from several distinct sources (sea level and tsunami runup data, eyewitness accounts, marine geophysical surveys, and paleo-geological investigations of undisturbed sediment cores inland from the coast) including numerical modelling of tsunami resonance behaviour. A comprehensive summary of local (travel time from 30 to 60 minutes) and regional (travel time from 2 to 3 hours) tsunami sources was compiled from available geophysical investigations (seafloor mapping and seismic profiling of faulting systems, underwater volcanoes and landslides) and knowledge of past volcanic behaviour.

Subduction interface earthquakes that originate from the Tonga-Kermadec-Hikurangi subduction zone (where the Pacific Plate underthrusts the Australian plate to the west) were identified as a major tsunami source for the region. This source area stretches from the eastern margin of North Island northward along the Kermadec Ridge toward Tonga. However, whether the entire subduction zone is a potential tsunamigenic hazard is not yet certain because of significant changes that occur in the crustal structure along this margin. Consequently further evaluation of potential tsunami generation from this source was suggested. Locations of this source together with six others (6) are illustrated in Figure 2.1-1.

Paleo-tsunami records with run-up elevations greater than 5 m were also reported. These reports identified at least five events that may have originated from local and regional sources. Further analysis of tsunami run-up height from paleo-tsunami deposits using numerical modelling incorporating detailed topography and nearshore bathymetry was suggested once credible source-generation scenarios have been constructed.

Numerical modelling of tsunamis was carried out using RiCOM software (Walters, 2005) with a focus on tsunami resonance behaviour caused by distant sources. Regular waves of constant height and specified period were used as initial conditions for the modelling. Different model simulations were run, covering a range of wave-train periods from 15 minutes to 5 hours. The sources were assumed from the eastern Pacific Ocean e.g. from South American. The model used relatively low-resolution bathymetry and topography data from GEBCO (2 arc minutes), with the results only applicable to open coastal areas, because the bathymetry data does not include estuaries. The broader pattern of resonance or amplifications was emphasized, however only model results for wave periods of 75 and 90 minutes were presented as the most relevant for the resonance of Bay of Plenty and Coromandel region. Local and regional sources were not included in this numerical modelling assessment.

The historic record shows that no locally or regionally sourced events have affected the BOP and EW region since 1840. However, at least 11 (eleven) far field tsunamis sourced mainly from South America are known to have affected places along the BOP and eastern Coromandel Peninsula. The historical record is recognised as being too short to cover large fault ruptures from local or regional sources, as they tend to have return periods of 200s to 1000s of years.

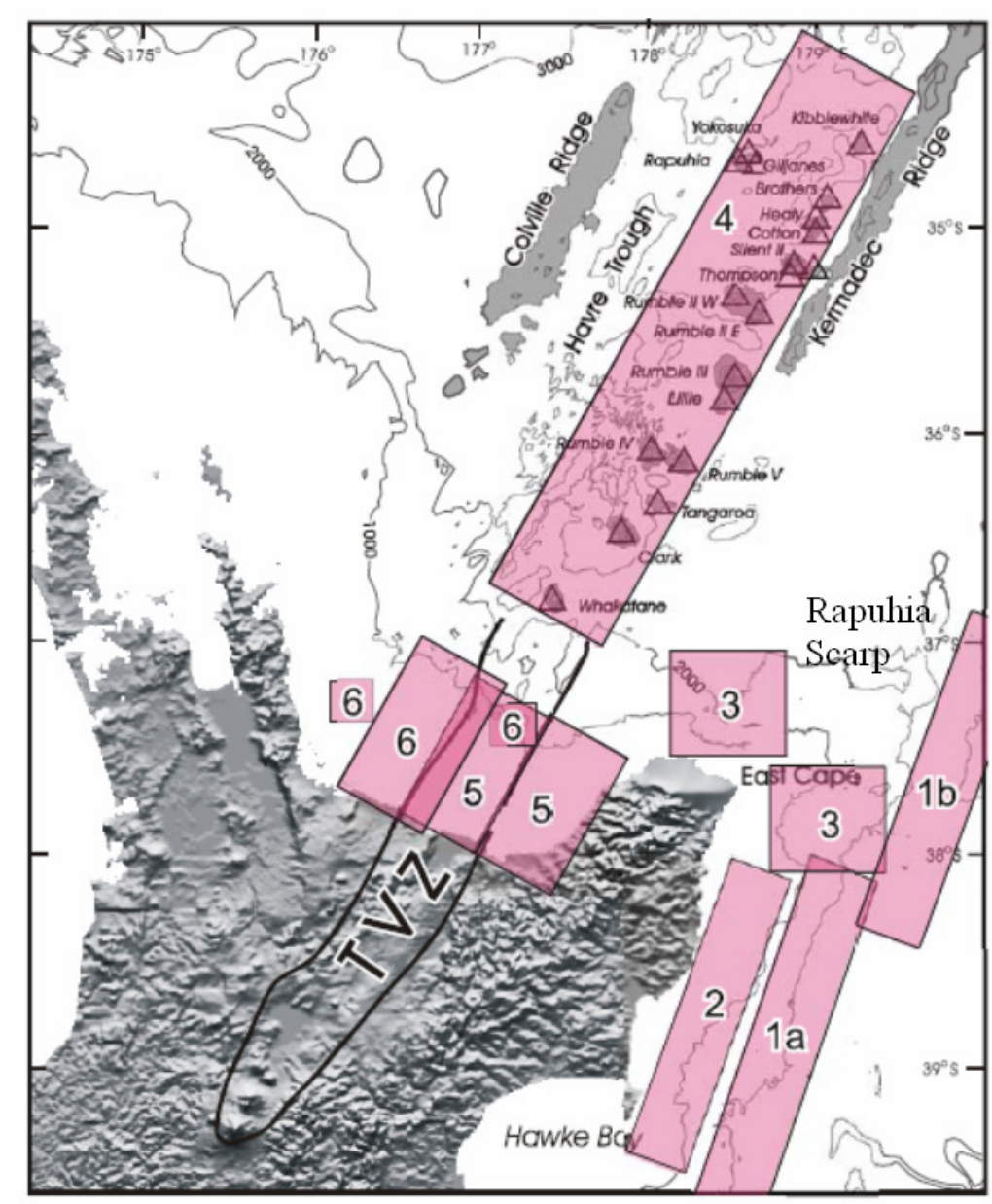

Figure 2.1-1 General locations of potential sources for regional and local tsunamis that could impact the Bay of Plenty and eastern Coromandel coasts correspond to a source along Hikurangi Margin, upper plate faults and landslides (1a, 2, 3), Tonga-Kermadec (1b), undersea volcanism along the Tonga-Kermadec system (4), local faults offshore from the Taupo Volcanic Zone – TVZ (5), and offshore volcanic island sources (6) (Source: Bell et al.2004).

Combination of historic records from AD1840 and paleo-tsunami signatures dating back 4000 years across the Eastern Coromandel and Bay of Plenty region show that a number of tsunami from both near and far field sources have affected the region (Table 2.1-1). These data show that no large local or regional source tsunamis have affected the Bay of Plenty or eastern Coromandel over the last 170 years. Potentially this could indicate that recurrence intervals for large earthquakes within this region are greater than 170 years. Paleo-tsunami sediment core records indicate that at least two major regional scale tsunami events occurred over the last 4000 years. One event was in AD1302-AD1435 with some evidence for two separate major events during this period, and an earlier event at 2500-2600 years BP.

Table 2.1-1 A summary of the known past tsunami events (updated from Bell et al. 2004).

Tsunami runup height (est.)	**<0.5 m***	**0.5-1 m**	**1-3 m**	**3-5 m**	**> 5 m**
No. of events	**>6**	**3**	**4-5**	**?**	**5 or 6**
Year(s)	June 2001	Feb 2010	May 1960		**Regional-scale**
	July 1998	Sept 2009	Aug 1883		AD1302-1435
	Oct 1994	Nov 1922	May 1877		2500-2600 y BP
	June 1977		Aug 1868		**Local-scale**
	Jan 1976		1700?		AD1600-1700?
	Mar 1964				AD1200-1300
					1600-1700 y BP
					2900-3000 y BP
* Many events of <0.5 m run-up may have occurred, but gone unnoticed before instrumental sea level records became available					
^ No events >3 m run-up in the historical records, and paleo-tsunami analyses at this stage can only resolve events with >5 m run-up					

2.2 Tsunami Source Study (Goff et al. 2006)

This study was undertaken by NIWA (Goff et al. 2006) to identify the most significant tsunami sources for the combined region (Northland Regional Council, Auckland Regional Council, Environment Waikato and Environment Bay of Plenty). General settings for each source (South American, Solomon Sea and New Hebrides areas, subduction zone event along the Tonga-Kermadec Trench, and selected local sources) were discussed.

Results were presented for the area encompassed by the four regional councils. Combination of an inverse solution (paleo-tsunami data guiding source selection) and source modelling was utilised to determine the most likely significant tsunami source

for the region. The results showed that a subduction zone event along the Tonga-Kermadec Trench represented the most significant tsunami source. In some cases, modelled surface water elevations at the coast were in excess of 10 m (Goff et al. 2006). Moreover, the report suggested that Mw 8.5 to 9.0 events on the Tonga-Kermadec Trench are not implausible based on paleo-tsunami data and the inverse modelling results. This was larger than possible magnitude from geophysical data at that time. Historical earthquakes of magnitude Mw 8.3 to 8.4 have occurred along the Kermadec boundary in the early 1900's (ITDB/PAC 2004).

The numerical model RiCOM (River and Coastal Ocean Model) of Walters (2005) was used to model tsunami generation and propagation. The model utilises Reynolds-averaged Navier-Stokes equations incorporating an incompressibility condition. However, hydrostatic approximation was used and the equations therefore reduce to non-linear shallow water equations. RiCOM uses a finite element grid with a time stepping algorithm in a semi-implicit numerical scheme. To represent inundation processes, a wetting and drying scheme is included and defined by the finite volume form of the continuity equation which calculates fluxes through the triangular element faces. To ensure that a model calculation is accurate and free from excessive numerical errors, the triangular elements are roughly equilateral in shape. Their size grading is smoothed from areas of high resolution (small grid size) in the coastal zone to low resolution (larger grid size) offshore. Several model grids were developed based on existing EEZ (Exclusive Economic Zone) data and GEBCO (IOC, IHO and BDOC, 2003) for the northern area.

For the Tonga-Kermadec source, the fault dislocation model of Okada (1985) was used to define the seabed displacement based on information derived from Pacheco et al.(1993). The report indicated that the magnitude and location of subduction zone events is not well defined for this region. Therefore, a range of events were used and the results compared with elevations of paleo-tsunami deposits, in this case, the 15th century event. However, details of faults parameters used for the range of scenario events modelled are not reported. A summary of the results is described as follows:

2.2.1 Event Mw 8.5

Events with magnitude Mw 8.5 were placed south and north of the Rapuhia Scarp (central), and further north at the boundary between the Kermadec and Tonga Trench at the point where the Louisville Ridge is subducted beneath the plate boundary as shown in Figures 2.2.1-1 to 3 (Figures 3.2.1 to 3.2.3 of the report). As previously mentioned, no detailed information was provided regarding fault parameters and dimensions except for the general subduction parameters sourced from Pacheco et al. (1993). Also, no information was provided on the model grid resolution used for the nearshore areas. Consequently, based on the figures contained in the report, model results are only applicable to open coastal areas as identified when the figures were enlarged (Figure 2.2.1-1 to 3).

2.2.1.1 Southern Section Scenario

This fault scenario is located south of the Rapuhia Scarp, off the East Cape Ridge. The model results show that the tsunami elevation pattern from this source mainly impacts the Bay of Plenty to Great Barrier Island (Figure 2.2.1-1). The modelled tsunami elevation pattern along the east coast of Eastern Coromandel Peninsula

ranged from 2 to 3 m. High concentration or maximum modelled tsunami elevation occurred around the Great Barrier Island.

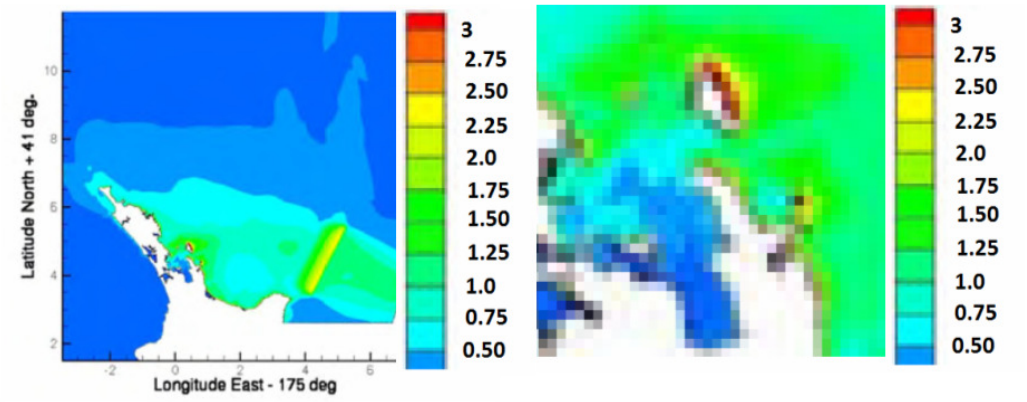

Figure 2.2.1-1 Modelled tsunami elevation resulting from a M_W 8.5 source located south of Rapuhia Scarp shows that the eastern Coromandel Peninsula is affected by tsunami with elevations at the coast (peak to trough) reaching between 2 to 3 m (Goff et al. 2006). The figure on the right shows that model is based on fairly coarse grid resolution. Scale bar unit is in metres.

2.2.1.2 Central Section Scenario

The central fault scenario source is located north of the Rapuhia Scarp. The modelling shows that this scenario generates less impact on the Eastern Coromandel coastline as most of the energy is focused on the Northland region. The range of modelled tsunami elevation patterns generated along the eastern Coromandel Peninsula ranged from 0.5 to 1 m with the highest wave energy concentrated around Great Barrier Island (2 m) as shown in Figure 2.2.1-2.

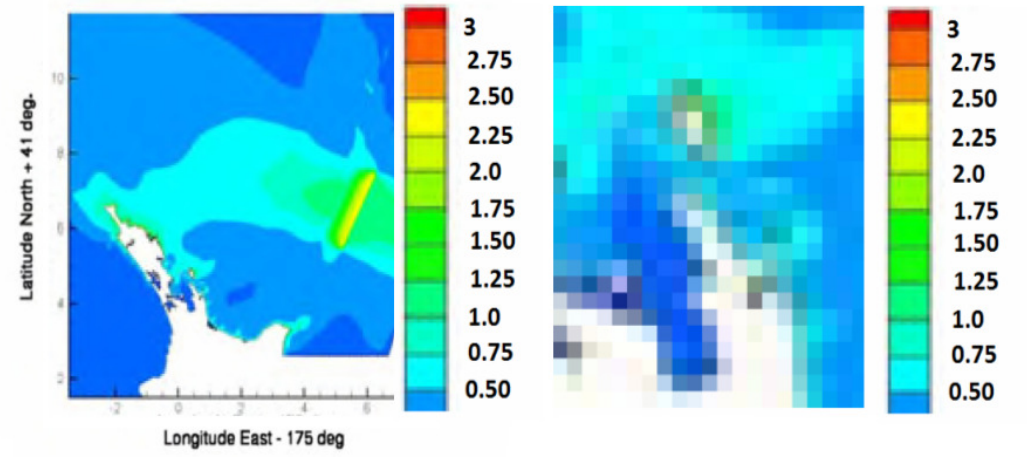

Figure 2.2.1-2 The modelled tsunami elevation produced by a Mw 8.5 event located to the north of Rapuhia Scarp shows that the eastern Coromandel Peninsula is less affected by tsunamis from this source as tsunami energy is concentrated farther north along Northland's coast. The figure on the right shows that the grid resolution is fairly coarse. The east coast of Coromandel Peninsula was affected by a tsunami with elevation at the coast (peak to trough) lying between 0.5 to 1 m (Goff et al.2006). However, the modelled tsunami elevation along the east coast of Great Barrier Island is still high (~ 2 m). Scale bar unit is in metres.

2.2.1.3 Northern Section Scenario

This fault section is located further north with its terminal point lying adjacent to the point where the Louisville Ridge is being subducted beneath the Australian Plate at 26°S. The model results showed that the tsunami elevation pattern from this source mainly impacts areas north of New Zealand. The modelled tsunami elevation patterns along the east coast of Eastern Coromandel Peninsula ranges from 0.5 to 1 m, with high tsunami elevation occurring around the Great Barrier Island ~ 2 m (Figure 2.2.1-3).

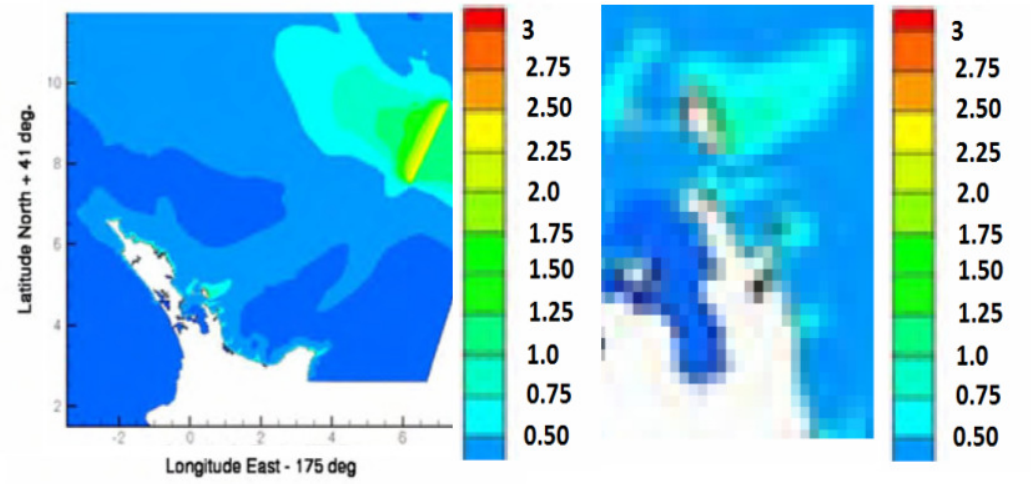

Figure 2.2.1-3 Modelled tsunami elevations resulting from a Mw 8.5 event from a source located further north shows that the east coast of eastern Coromandel Peninsula is less affected by tsunami, as the main tsunami energy is directed to the northwest of NZ (Figure left) perpendicular to the fault plane. The modelled tsunami elevation (peak to trough) along the east coast of the Coromandel Peninsula is between 0.5 to 1 m (Goff et al.2006), except for the east coast of Great Barrier Island (~ 2 m) as indicated in the Figure on the right. The grid resolution is fairly coarse. Scale bar units are in metres.

The report shows that the greatest effect of tsunami generated from Mw 8.5 scenarios along the eastern Coromandel Peninsula was due to sources located south of Rapuhia Scarp while sources from central and further north, provided lesser impacts.

2.2.2 Event Mw 9.0

The report indicates that even though a magnitude of Mw 8.0 to 8.5 is considered a reasonable estimate for the maximum magnitude event for the Tonga-Kermadec subduction zone, an Mw 9.0 event was included as the Boxing Day 2004 event suggests that those magnitudes (Mw 8.0 to 8.5) probably underestimates the potential maximum magnitude that could occur.

The magnitude Mw 9.0 scenarios were placed at south of the Rapuhia Scarp, across the scarp and further up to the north. The fault length and slip was twice that of the Mw 8.5 scenario. However, detailed fault information was not provided in the report. The model results based on these scenarios are illustrated in Figure 2.2.2-1 to 3 (Figures 3.2.4 to 3.2.6 of the report).

2.2.2.1 South Rapuhia Scarp Scenario

This source extends from the East Cape Ridge NE towards the Rapuhia Scarp (N15^o E trending) following the subduction zone trend. The modelled tsunami elevation results obtained from this source indicate that the tsunami significantly impacts the entire shoreline from the Bay of Plenty through to Great Barrier Island, while the impacts lessen further to the north. Modelled tsunami elevations along the east coast of eastern Coromandel Peninsula range from 3.5 to 5.5 m as shown in Figure 2.2.2-1, with tsunami waves focusing along the east coast of Coromandel Peninsula. The east coast of Great Barrier and Mercury Islands experiences the maximum tsunami elevation of ~ 5.5 m. However, no information can be derived for harbour and estuaries along the east coast as the grid size used in the model was too coarse (Figure 2.2.2-1 right).

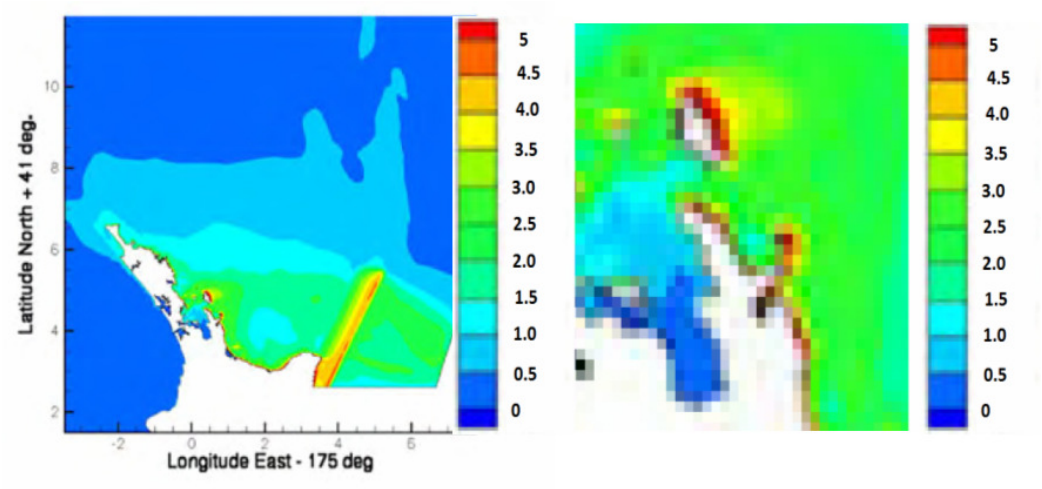

Figure 2.2.2-1 The modelled tsunami elevation resulting from a (Mw 9.0) source, extending from the East Cape Ridge northeast across the Rapuhia Scarp, shows significant tsunami impact along the east coast of the Coromandel Peninsula. Tsunami impacts most of the eastern coastline with a model tsunami elevation at the coast (peak to trough) between 3.5 to 5.5 m (Goff et al. 2006). High concentrations of tsunami waves occur along the east coast of Great Barrier and Mercury Islands. Figure on the right shows the grid resolution was fairly coarse. Scale bar unit is in metres.

2.2.2.2 Central Location across Rapuhia Scarp Scenario

This source located immediately offshore of the East Cape Ridge extends to the northeast across the Rapuhia Scarp along the N15^{o}E trending Hikurangi trench as illustrated in Figure 2.2.2-2 (left). The tsunami elevation results modelled from this source show significant tsunami impacts along the entire east coast from the Bay of Plenty up to Northland. The modelled tsunami elevations ranged from 2 to 5.5 m with elevation patterns showing that the Coromandel Peninsula (including the east coast of Great Barrier and Mercury Islands) experiences maximum wave elevations ranging from 4 to 5.5 m (Figure 2.2.2-2, right). Again, grid resolution is too coarse near to the coast to model tsunami elevation inside the harbour and estuaries (Figure 2.2.2-2 (right)).

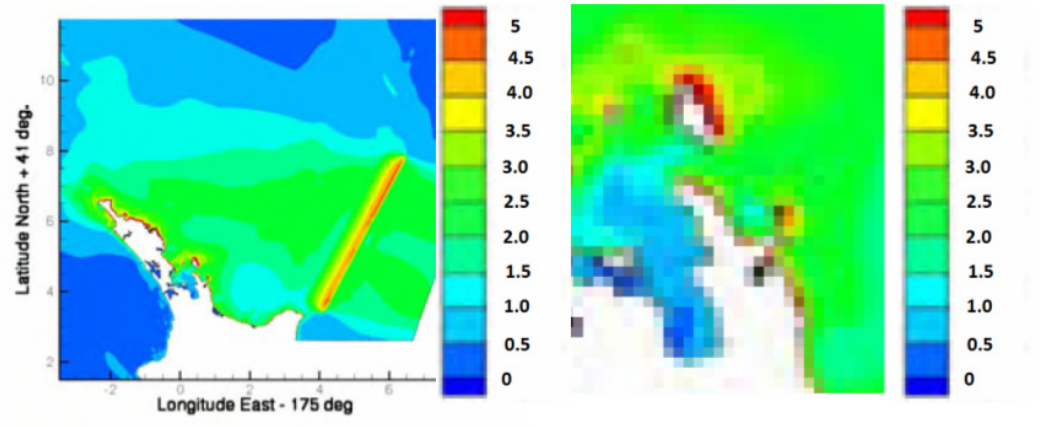

Figure 2.2.2-2 This tsunamigenic earthquake scenario with a magnitude of Mw 9.0 is located immediately offshore of East Cape Ridge and extends northeast across Rapuhia Scarp. It produces a tsunami elevation (peak to trough) of 4 to 5.5 m along the eastern Coromandel coast (Goff et al. 2006). The highest tsunami elevation occurred along the east coast of Great Barrier Island (Figure right). The grid resolution is too coarse to assess the tsunami elevation and pattern inside the bays, harbour and estuaries. Scale bar units are in metres.

2.2.2.3 Northern Scenario

This source region is located to the north of Rapuhia Scarp, extending from the scarp to the northeast (N15°E trending) to the point where the Louisville Ridge intersects the Hikurangi Trench at 26°S. Modelled tsunami elevation results from this source show that most of tsunami energy is directed to the northwest perpendicular to the fault plane with less energy directed to the eastern Coromandel Peninsula. The modelled tsunami elevation along the east coast of eastern Coromandel Peninsula lies between 1 and 3 m, with the highest tsunami elevation occurring around Great Barrier and Mercury Islands (Figure 2.2.2-3).

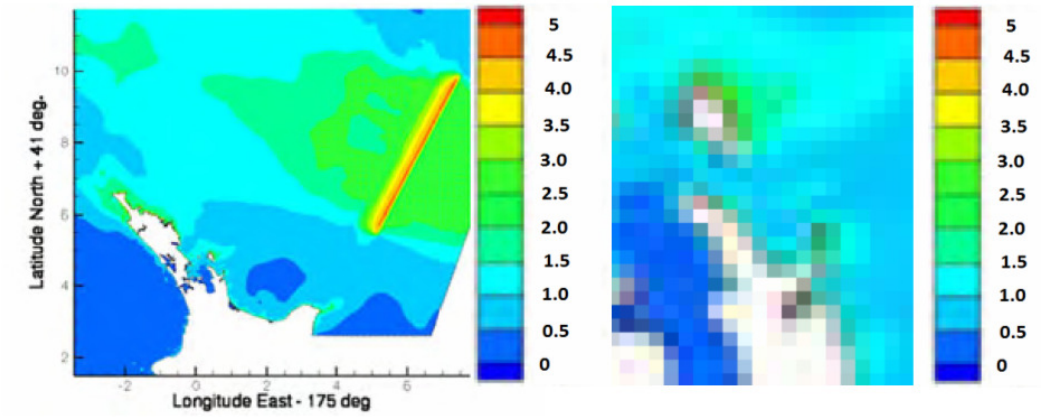

Figure 2.2.2-3 Relatively lower tsunami impacts occurred along the eastern Coromandel coast from this northern source. Tsunami elevations at the coast (peak to trough) ranged between 1 to 3 m (Goff et al. 2006) with the highest tsunami elevation occurring along the east coast of Great Barrier and Mercury Islands. The figure on the right shows a fairly coarse grid resolution. Scale bar units are in metres.

2.2.2.4 Summary

From the Mw 8.5 and M 9.0 scenarios, the report concluded that the east coast of eastern Coromandel Peninsula is highly affected by tsunamis generated from the south and central region of Tonga-Kermadec subduction zone as illustrated in Figure 2.2.2-4 (Figure 4.3.2-1 of the original report Goff et al. 2006). This Figure was derived from modelling using a higher grid resolution that allowed modelled tsunami elevations along the coast and inside the Mercury Bay to be shown. The distributions of tsunami elevation along the coast from these sources have a similar pattern and magnitude to that shown by paleo-tsunami deposit data of Goff et al. 2005.

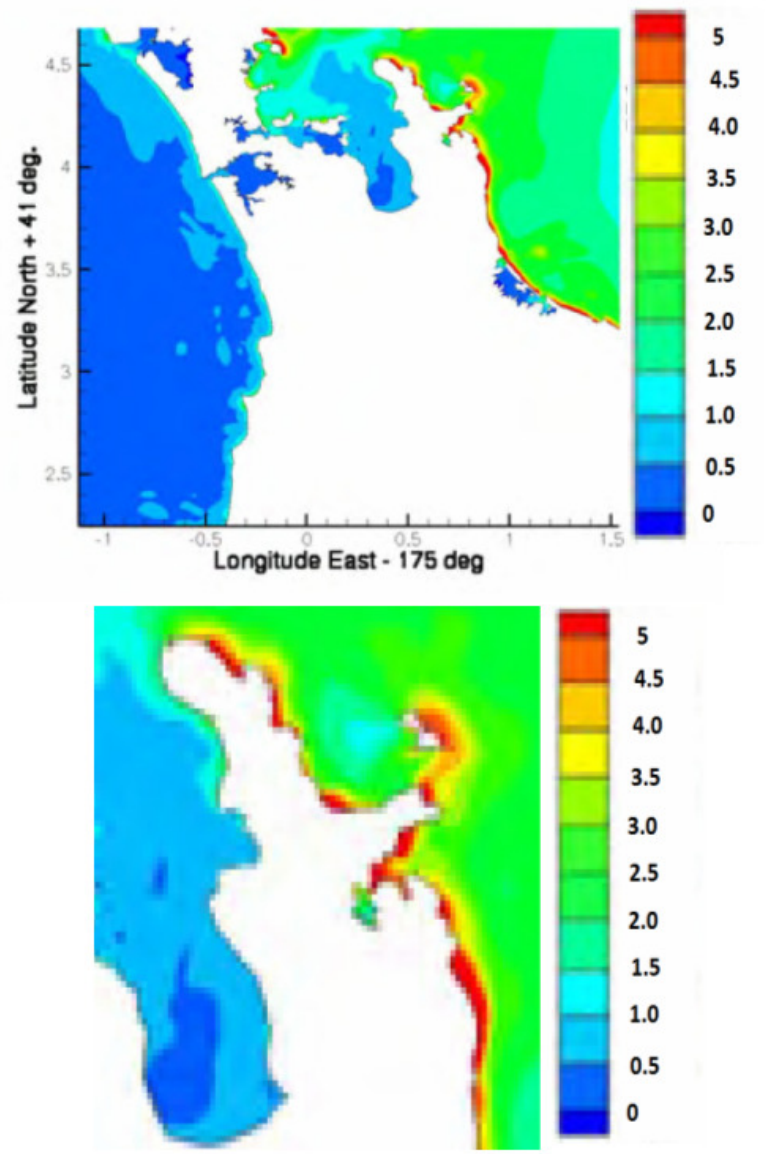

Figure 2.2.2-4 Distribution of tsunami elevations along the east coast from a Mw 9.0 event on the south-central part of Tonga-Kermadec Trench shows a similar pattern and magnitude as paleo-tsunami deposit data from Goff et al. 2005 for tsunami elevations ~ 5 m. Scale bar unit is in metres.

3.0 TECTONIC SETTING AND SEISMICITY OF TONGA-KERMADEC TRENCH

The Hikurangi-Tonga-Kermadec subduction zone is located in the Pacific Ocean to the northeast of New Zealand, as a result of the Pacific Plate being subducted below the Indo-Australian and Tonga Plates (Figure 3.0-1). This extended Australia-Pacific plate boundary reflects a multistage tectonic history related to global rearrangements of plate convergence in the Southwest Pacific (Bonnardot et al. 2007). The lateral variation of the subduction zone is continental in character along the Hikurangi Trench where the overriding continental Australian Plate forms the North Island of New Zealand. It transitions to an island arc in the north along the Kermadec – Tonga Arc. This lateral variability involves changes in volcanic and hydrothermal activity, a transition from accretion to subduction zone erosion, back arc rifting and spreading as well as increasing seismicity northward (Scherwath, et al. 2008).

The Tonga-Kermadec subduction zone with an overall length of nearly 2700 km (extending from 38°S to 15°S) is characterised by a N15°E trending back-arc domain that mostly parallels the volcanic arc. This back-arc domain exhibits strong variations in stress and orientation of tectonic structures from north to south (Bonnardot et al. 2007). The Louisville Ridge Seamount Chain (LRSC), is subducted obliquely relative to the trench, and intersects what can be described as a decoupled arc at 26°S. The LRSC divides the subduction zone system into two distinctive back-arc basins: the Lau Basin, which is characterised by back-arc spreading to the north, and the Havre Trough, which is dominated by back-arc rifting in the south (Bonnardot et al.2007 and Karig, 1971). The trench to the north of the LRSC is known as the Tonga-Trench (~1200 km long), and to the south as the Kermadec Trench (~1500 km long). The rates of southward movement of Pacific plates relative to Australian Plate are 8.5 cm/year at 17°S, 7 cm/year at 27°S and 5.5 cm/year at 35°S (Figure 3.0-1).

3.1 Distribution of shallow seismicity and focal mechanisms

Bonnardot et al. (2007) on the basis of shallow seismic activity distributions divides the Tonga-Kermadec subduction zone into three domains that correspond to the principal tectonic units (i.e., the interplate zone, the arc-back arc domains and the north-western area) as illustrated in Figure 3.1.1. The focal mechanism solutions (CMT) and the Engdahl catalogue of shallow seismicity with earthquake depth < 50 km were used to model the shape and state of stress of the slab. Three groups based on the P- and T-axis dip were derived along the subduction zone. These are: the reverse group (T-axis dip $\geq$ 45°), the normal group (P-axis dip $\geq$ 45°) and the strike-slip group (P and T-axis dip < 45°) (Figure 3.1-1). Four domains with preferential types of faulting were derived: (zone a) the interplate area, (zone b) the Kermadec-Havre domain, (zone c) the Tonga-Lau domain and (zone d) the large northern part of the Lau Basin. It is clear from Figure 3.01 that the thrust events dominate the interplate areas with few normal events, while normal events dominate the interplate areas near the Hikurangi Plateau and East Cape Ridge.

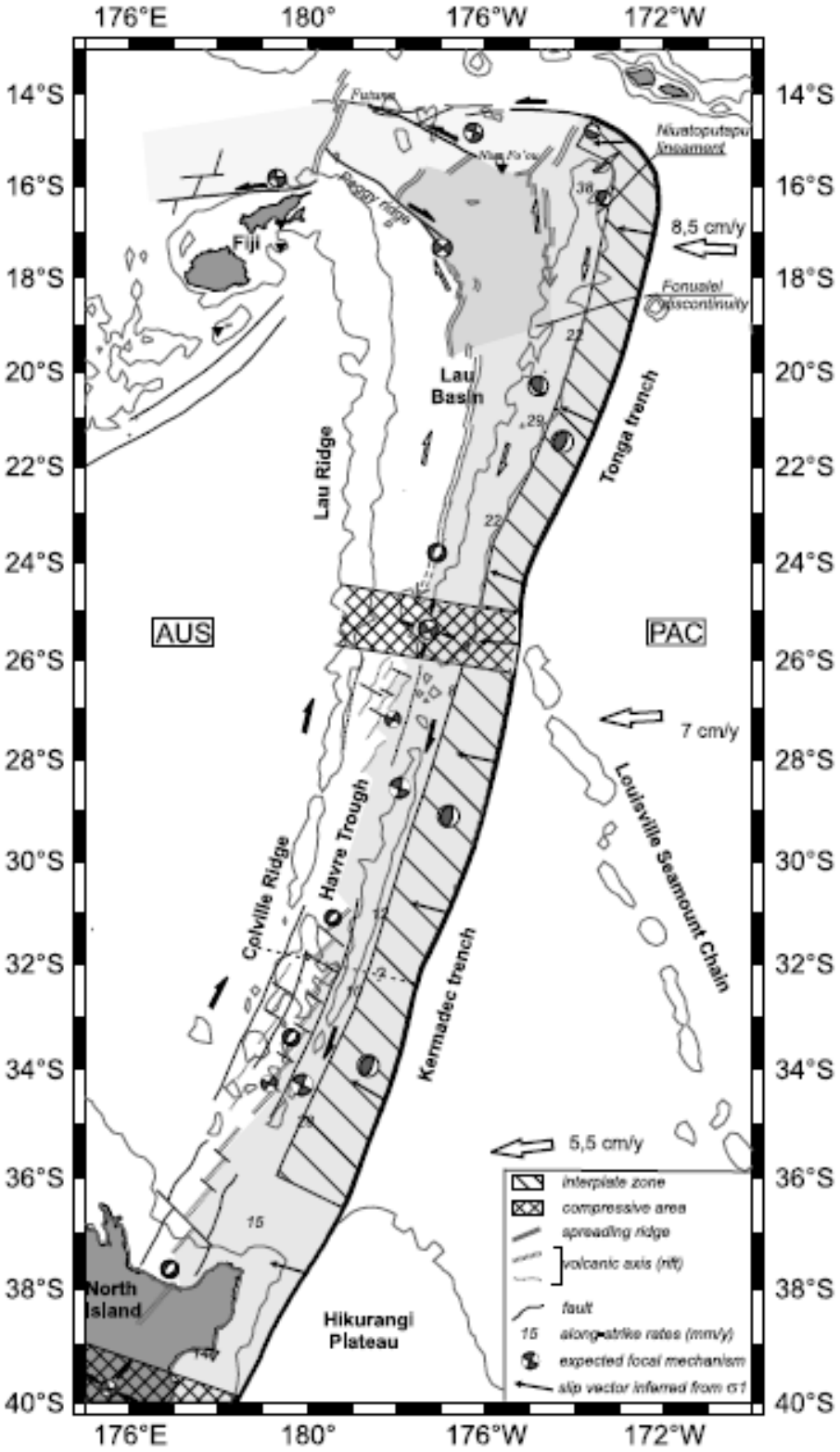

Figure 3.0-1 Tectonic setting of Tonga-Kermadec Trench showing principal tectonic units and expected earthquake focal mechanism from Bonnardot et al. 2007. PAC = Pacific Plate, AUS = Australia Plate.

The interplate area (Figure 3.1-1 - zone a) provides the main focus for analysis of the tsunamigenic region along this subduction zone. This domain lies between the modern volcanic arc and the trench, and is the most active zone in the Tonga-Kermadec system (Bonnardot et al. 2007) where the under-thrusting of the subducting Pacific plate provides the dominant mechanisms driving seismicity within this region.

Bonnardot et al. (2007) demonstrates the importance of seismic gap features along this interplate zone that segment the N15°E trending interplate zone. This may reflect different seismic cycling occurring along this interplate zone. Two large gaps, which are localised in front of the LRSC and the Hikurangi Plateau respectively, were identified at 25-27°S and 33-40°S. These topographic highs were expected to increase the interplate coupling that eventually locks the subduction zone and may strongly disturb the stress regime in the upper plate as interpreted previously by Scholz and Small (1997). Watts et al (2010) identified the gap at 25-27°S as being ~ 170 km long, and characterised by shoaling of the trench due to the intersection of the LRSC and the subduction zone at 26°S. Based on Scholz and Small (1997), the gap is locally well-coupled and seismically locked. Furthermore, Watts et al (2010) have suggested that Mw>8.0 earthquakes are possible in the future for this gap as it has sufficient slip length to generate events of this magnitude. This was also identified previously by Christensen and Ruff, (1988). They suggested that these two gaps have the potential for future large under-thrust events.

Based on their calculations and observations, Scholz and Small (1997) support the idea of Cloos (1992) and Christensen and Lay (1988) that seamount subduction will enhance local seismic coupling. However, Watt et al (2010) suggests that seamount subduction is linked in some way with the seismicity of convergent plate boundaries that either promotes large earthquakes or simply holds them up until the next one occurs. Other smaller seismic gaps centred roughly at 18°S were also identified. One gap is located in front of a seamount that has not yet been subducted (Bonnardot et al. 2007) and another one exists further south. The Samoa Earthquake (Mw 8.0) and tsunami on September 2009 may be related to this seismic gap. However, further analysis needs to be carried out.

The large gap at 33-40°S is poorly constrained due to small numbers of earthquakes along this section of the subduction zone (Bonnardot et al.2007). Following Collot and Davy (1998), the gap is associated with the initial collision point between the Hikurangi plateau and the Kermadec Trench. The northern edge of the plateau is known as Rapuhia Scarp. This scarp may act as a termination point for the subduction zone rupture to the north and south, and the change in fault dip across the Scarp suggests that surface deformation caused by the fault rupture my vary between sections to the north and south of the scarp (Bell at al. 2004). The scarp is 1 km high resulting in an increase in depth of approximately 1.5 km to the north. The steep slope of the shelf has the potential to produce large submarine landslides and slumps.

Geometric variations of the subducting slab at four locations along the Tonga-Kermadec trench were defined by Bonnardot et al, 2007 (Figure 3.1-2) using the Bossu (2000) statistical method that showed the variation of slab dip for both shallow dip, α, (< 50 km) and deep dip, β, (>50 km) with precision $\pm$ 5^{o}. The results showed that shallow dip angles (< 50 km) varied from 16^{o} to 31^{o}. The seismic gaps are observed in zones where the slab dip at the interplate contact is lower (α=16-18^{o} $\pm$5^{o}) suggesting strong interplate coupling (Bonnardot et al. 2007). In comparison Pacheco et al. 1993 derived a dip angle of 28^{o} for the Kermadec trench from 26^{o}S to 37^{o}S (1185 km in length).

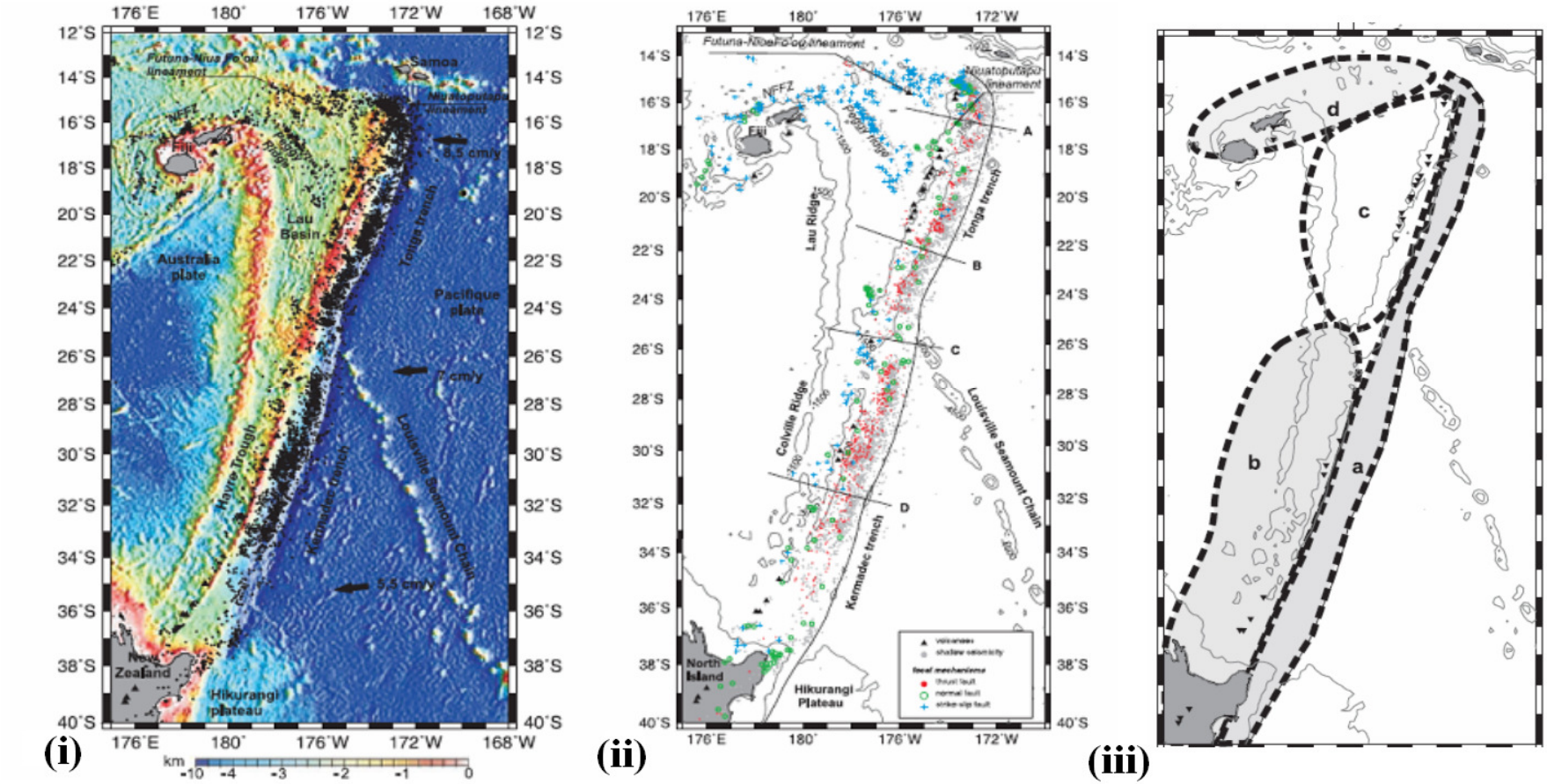

Figure 3.1-1 Plate tectonics of Tonga-Kermadec Trench showing (i) distribution of shallow seismicity (<50 km) and focal mechanisms (ii) four domains based on principal tectonic units (iii): zone a, Interplate zone; zone b, Kermadec-Havre Trough zone; zone c, Tonga-Lau zone; and zone d, northern area (Bonnardot et al.2007). Lines A, B, C and D shown in (ii) are the slab cross section lines illustrated in Figure 3.1-2.

This page is intentionally left blank.

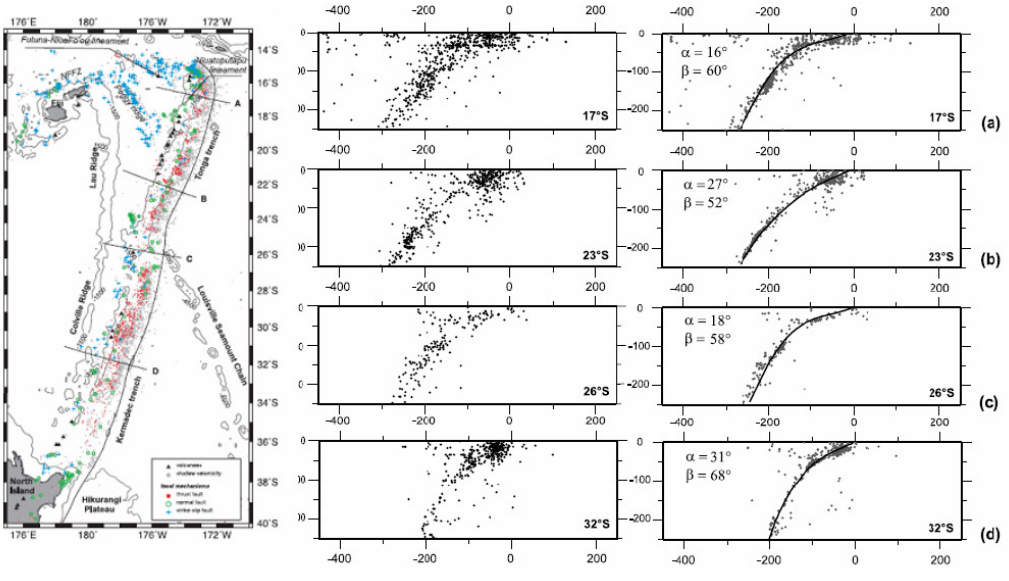

Figure 3.1-2 Cross sections of global seismicity with the cross sections width of 600 km based on the Engdahl catalog (Engdahl et al., 1998) along lines A, B, C and D which relates to 17°S (a), 23°S (b), 26°S (c) and 32°S (d) respectively that show the variation of shallow slab dip, α (<50 km) and the deep slab dip, β (>50 km) with ± 5° precision (Bonnardot et al.2007).

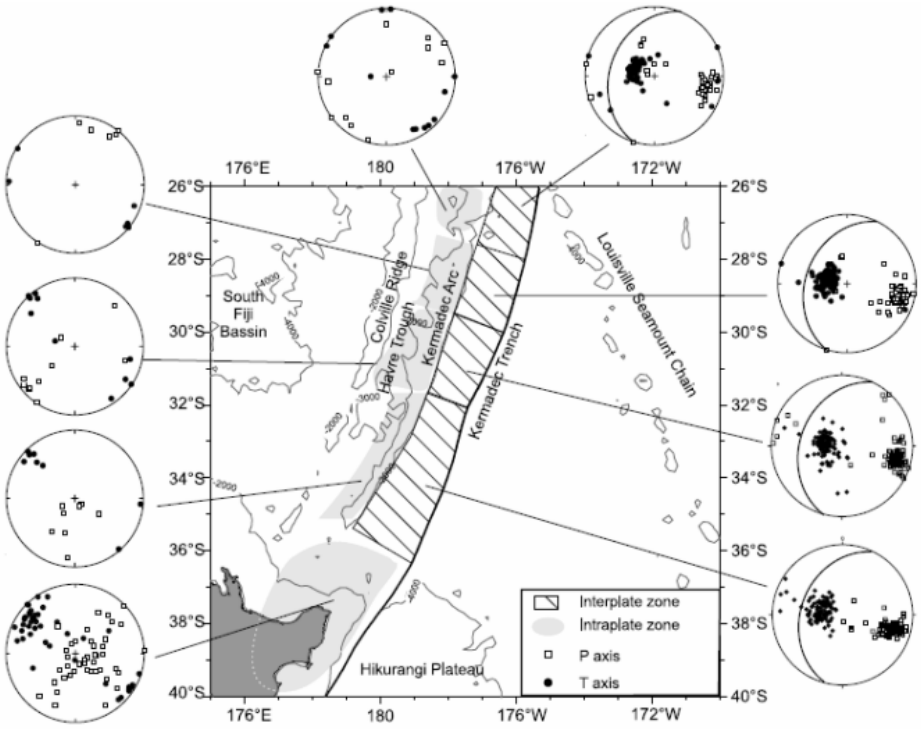

Figure 3.1-3 Orientations of P- and T- axis's for selected areas in the Kermadec subduction zone. Some areas were poorly constrained owing to a small number of earthquakes (map source: Bonnardot et al. 2007).

3.2 Trench sediment, subducted plate age, convergence rate and seismic coupling

The seismic coupling coefficient is used to describe the locking condition of the subducted plate. It is the ratio of the slip rate determined from the occurrence of large earthquakes to the total slip rate (seismic and aseismic). Based on observed and computed seismic coupling worldwide, Pacheco et al. 1993 found no significant correlation between the seismic coupling coefficient and the width of the seismogenic zone or other subduction parameters such as the age of oceanic lithosphere that is being subducted, plate convergence rates and absolute velocity of the upper plate in the fixed hot spot reference frame. They explained the variation in seismic coupling observed as being caused by differences in the frictional behaviour of materials at the plate interface, such as the subduction of large bathymetric features, topographical roughness, and sediment composition.

For the Kermadec trench (from 26°S to 37°S), Pacheco et al.1993 showed that the computed seismic coupling associated with a cumulative moment magnitude Mw 8.1 is 0.160 based on 90 years of seismicity (1900-1990), while seismic coupling based on slip prediction models lies between 0.21 to 0.29. Aseismic motions are possibly common along this subduction zone, however on October 20, 1986 an earthquake with magnitude Mw = 8.1 occurred with its epicentre located at 28.12°S, 176.37°W (south of the LRSC) (Lundgren et al. 1989) indicating that this region is not completely aseismic.

Ruff (1989) emphasized that sediments do significantly impact geology, geochemistry, and geophysics as many geological terranes are thought to be exhumed trench sediments. Recycling of crustal material via sediment subduction affects the geochemical evolution of the mantle. Sediments may also influence subduction zone seismicity. Ruff (1989) suggested a correlation between great earthquakes and excess trench sediment as an addition to the previous identified relationships between age of subducting plates and convergence rates (Ruff and Kanamori, 1980). Based on 19 great earthquakes (Mw>8.0) along the subduction zones of South America – Aleutian – Kamchatka and Japan in combination with world trench sediment classification of Hilde (1983), he showed that most of the largest earthquakes occur in regions where excess sediment exists with the exception of the two great Aleutian earthquakes.

These two great Aleutian earthquakes occurred in a subduction zone dominated by horst graben structures (HTS) (Figure 3.2-1). HTS potentially generate large earthquakes even though they occur less than excess trench sediment (ETS) in subduction zones. Observations also showed that many zones with ETS have not been subject to great earthquakes so it seems that ETS does not necessitate these events. Also the Ruff and Kanamori (1980) rule indicating that great earthquakes tend to occur in subduction zones with faster convergence and younger lithosphere was violated during the Boxing Day 2004 mega thrust event. Here the lithosphere is old and subducts slowly (McCaffrey, 2008). So perhaps the occurrence of this mega event may be better explained by the role played by ETS than just its presence.

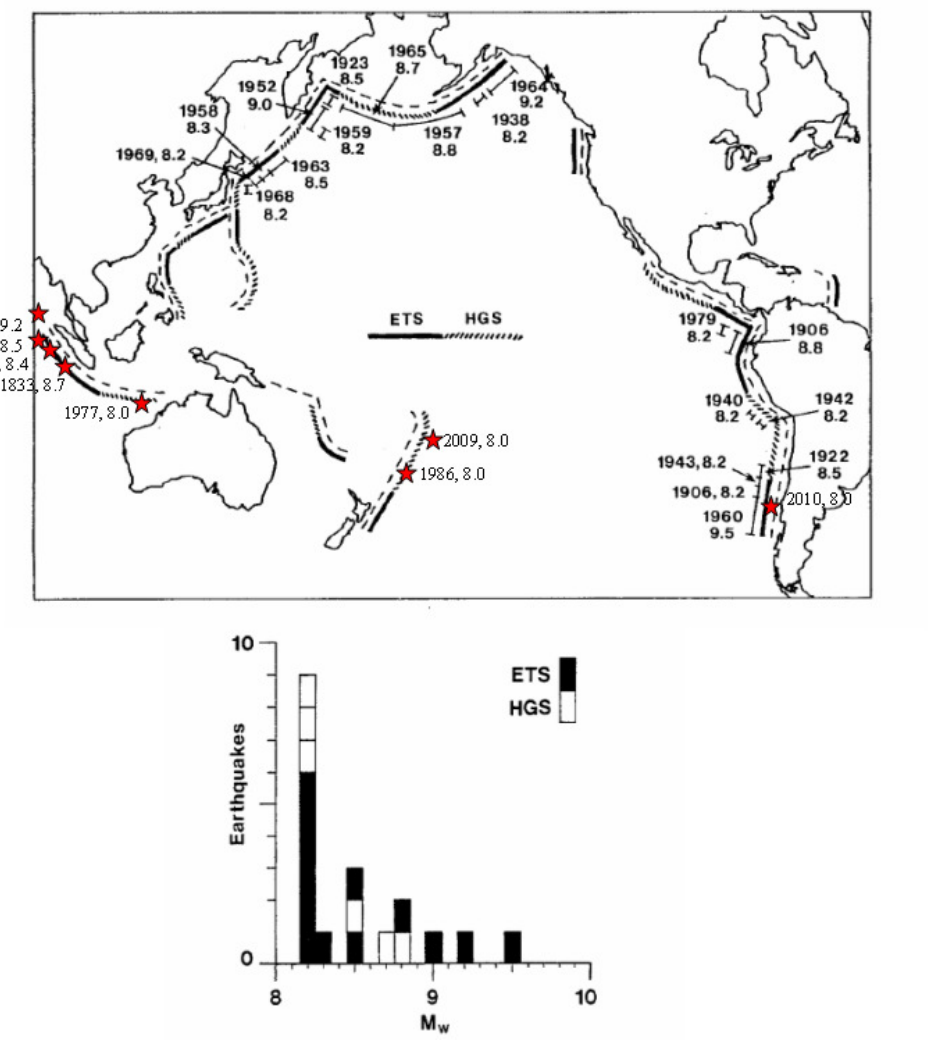

Figure 3.2-1 The location of excessive trench sediment (ETS) and horst graben structures (HGS) in relation to large earthquakes occurring from the 1900's shows that most large earthquakes occur along trenches with excessive sediment. However, large earthquakes with magnitude up to M=8.8 are also possible for horst graben structures that can generate devastating tsunamis as occurred in 1957 and 1965 in the Aleutian arc, Sumba in 1977 and Samoa 2009. Red stars shows large earthquakes occurring since the 1900's not plotted on the original map of Ruff (1989).

Ruff (1989) suggests a physical mechanism that addresses this role. He speculates that excess sediments subducted as a coherent sedimentary layer at elevated temperature and pressure forms a homogenous and strong contact zone between the plates. This contact zone was later explained by Fuller at al. (2006). Fuller et al. used recent observations of an association between forearc basins and slip during subduction-zone thrust earthquakes to suggest a link between processes controlling upper plate structure and seismic coupling on the subduction-zone thrust fault. Their numerical simulations demonstrate the role of trench sediment in stabilising the underlying wedge, thereby preventing internal deformation beneath the basin. This allows maximum slip to occur during great-thrust earthquakes in situations where sedimentary basins stabilize the overlying wedge. Their results show that due to the lack of deformation in stable sedimentary basins, there is an increased likelihood

of thermal pressurization of the subduction thrust, which allows the fault to load faster, and allows greater healing of the fault between rupture events.

The trench sediment distributions along the Tonga-Kermadec Trench (Figure 3.2-1 – based on Hilde, 1983) define areas of excess trench sediment occurring along the Hikurangi trench up to the Rapuhia Scarp and then continues to the north with horst and graben structures.

Given the above explanations, these areas are also capable of generating large earthquakes as pointed out by Nishenko and McCann (1981) based on 1833 event. Indeed, several large earthquakes have occurred along the Tonga Trench in 1982 and 1995 (Ms = 7.7 and 8.1), and Kermadec Trench 1986 (Ms = 8.1-8.3). The 1982 and 1986 events occurred on both side of the LRSC, while the 1995 event occurred at the corner of Tonga Trench. The recent events of September 2009 (Mw = 8.0) are a couplet (Beavan et al. 2010, Lay et al. 2010, Satake 2010) that was located further north of 1982 event, south of the 1995 under-thrusting event and further east of the 1986 normal event.

These recent events generated devastating tsunamis in Niautaputapu Island (Tonga) and Samoa Island. Small tsunamis were also recorded at NZ tide gauges along the east coast of North Island. These vigorous seismic activities along the Tonga trench and near the LRSC were not followed by any increase in activity along the southern extent of the trench (Kermadec trench). The Kermadec trench section remains quiescent with no large earthquakes occurring over the last 170 years, leaving a large seismic gap with significant implications for the region.

4.0 FREQUENCY- MAGNITUDE AND EARTHQUAKE PREDICTION

4.1 Frequency-magnitude of the earthquake along the Kermadec Trench

The International Tsunami Data Base (ITDB/PAC2004) which also incorporates the NOAA/NESDIS/NGDC data set is used in estimating the frequency-magnitude of earthquake occurrence along the Kermadec Trench. The spatial and temporal distribution plot of all earthquakes within the Kermadec and Havre-trough zone and their frequency magnitude relationship are plotted in Figure 4.1-1. The spatial and temporal distribution of shallow earthquake of less than 50 km depth and magnitude of greater than Ms = 7.0 are plotted in Figure 4.1-2.

The temporal distribution plot of the earthquake based on the ITDB/PAC 2004 data base (from 1900 to 2004) (Figure 4.1-1 b) shows that more earthquakes were recorded since the 1960's. This is due to improvements in seismological observations for the region rather than to higher seismic activity. The temporal distribution also shows that there is a gap in the record from 1917 to 1943 where no earthquakes (large or small) were recorded. This period coincides with the time between the two World Wars.

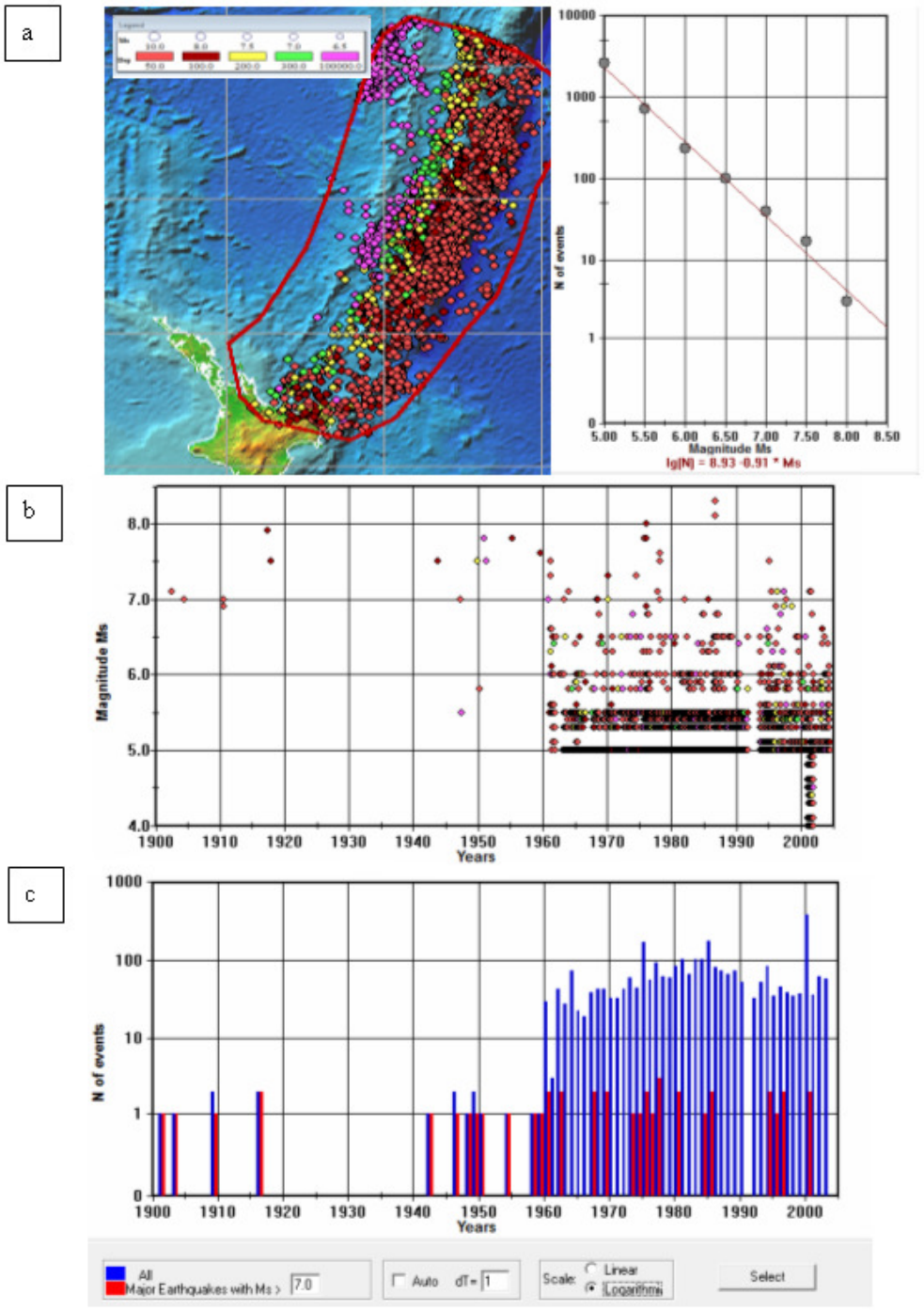

Figure 4.1-1 Spatial (a) and temporal (b) distributions of earthquakes greater than MS = 4.5 within the Kermadec subduction zone and the Havre Trough zone. There is a gap where no seismicity was recorded in between 1917-1943 (b, c). There are 41 earthquakes with magnitudes greater than Ms = 7.0 (red bar) (c). (Data source: ITDB/PAC2004).

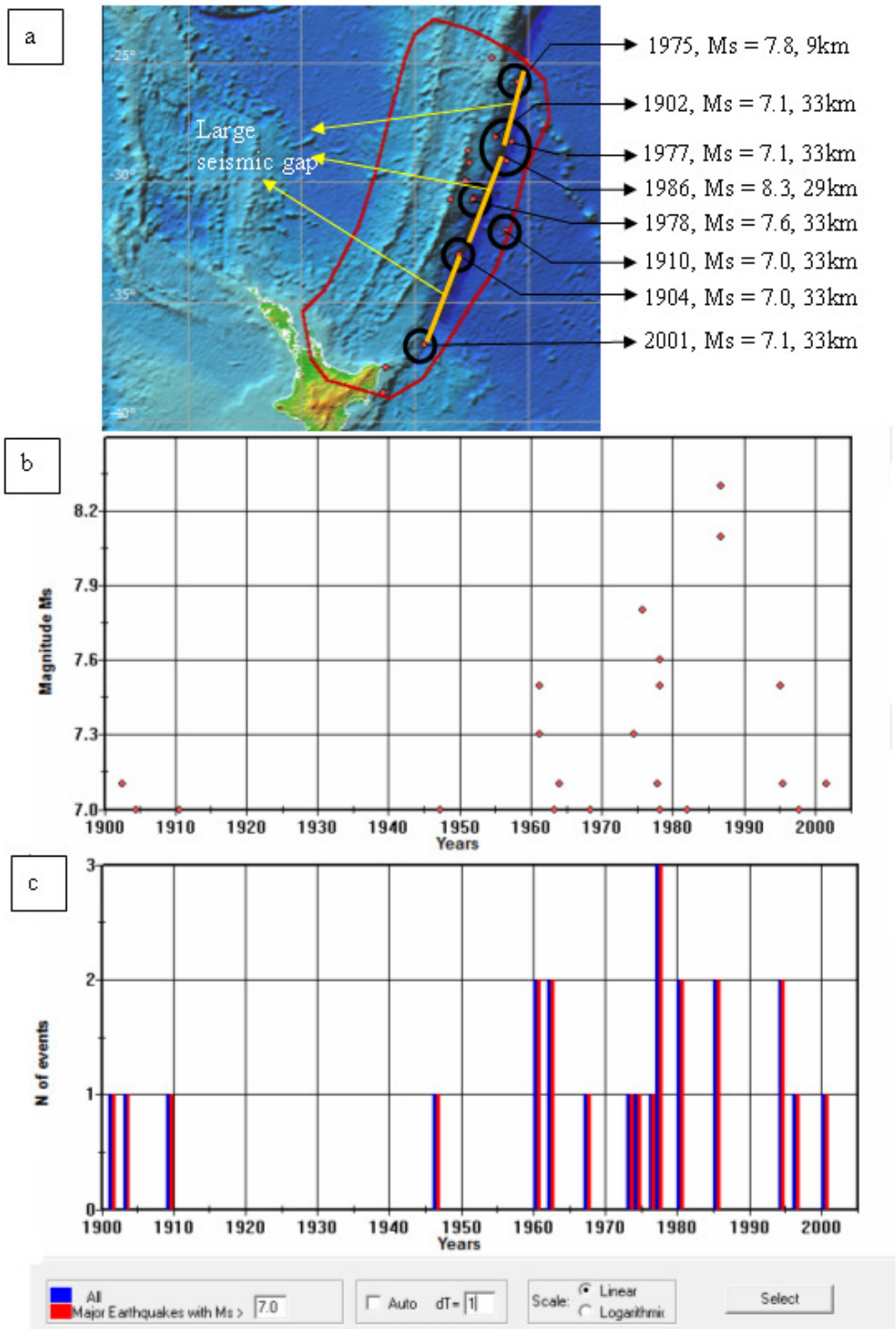

Figure 4.1-2 Spatial (a) and temporal (b) distribution of large shallow earthquakes greater than M_S = 7.0 and depth less than 35 km. These events occur mostly within the interplate zone (along the subduction zone). There is a gap between 1917-1943 where no seismic activity has been recorded (b, c). This gap coincides with the inter-world war period. There are 24 earthquakes with magnitude greater than Ms = 7.0 (red bar) (c). (Data source: ITDB/PAC2004).

The database shows that a total of 2788 earthquakes occurred within this zone with magnitudes ranging from Ms = 4.5 to 8.3 during the period 1900 – 2004, 41 of which had magnitudes greater than Ms = 7.0, or nearly 1 event every 3 years. Among the 41 earthquakes, 24 of them are generated along the Kermadec trench with depths less than 35 km, or within the interplate zone. This gives nearly 1 event every 5 years. The largest event occurred in 1986 near to the northern end of the Kermadec trench (near to the LRSC intersection). The last large event along the Kermadec trench occurred in 2001 near to the southern end of the Kermadec trench (Figure 4.1-2 a). This figure clearly shows several seismic gaps along the Kermadec Trench that are consistent with the data set used by Bonnardot et al.2007.

4.2 Long-term earthquake prediction

Papadimitriou (1994) acknowledges that the concept of seismic gap as applied to various regions of the world over the last few decades provides a means for forecasting large earthquakes. However, usable information is limited by the location and maximum magnitude of recorded events. The use of repeat times in estimates of seismic potential and better forecasts of large shock events also provides uncertainties which in some cases are very large due to the shortness of the record. This record often does not include even one complete cycle of large earthquakes.

Long-term prediction of large shallow earthquakes along the Tonga-Kermadec seismic zone has been assessed by Papadimitriou (1994) based on the time- and magnitude-predictive model of Papazachos and Papaioannou (1993). Papadimitriou (1994) defined three-seismogenic sources along the Kermadec arc using the arc segmentation of Nishenko (1991) described as the North Kermadec (source 5), Central Kermadec (source 6), and South Kermadec (source 7) as illustrated in Figure 4.2-1. All earthquakes with magnitudes Ms >7.0 during the time period of 1897-1992 are used to obtain the predictive relationship:

$$\text{Log } T_t = 0.09M_{min} + 0.43M_p - 0.41 \log M_o + 8.08,$$

with a correlation coefficient equal to 0.61 and standard deviation ~ 0.25. The empirical relationship for the magnitude of the following mainshock is as follows:

$$M_f = 0.71M_{min} - 0.20M_p + 0.47 \log M_o - 8.37.$$

T_t is the inter-event time, measured in years, M_{min} the surface wave magnitude of the smallest mainshock considered, M_p the magnitude of the preceding mainshock, M_f the magnitude of the following mainshock, M_o the moment rate in each source per-year. As there is a considerable fluctuation of the observed repeat times (T) and the corresponding repeat times given by the empirical relation (T_t), Papadimitriou (1994) suggested that it was better to determine the probability of occurrence of an earthquake larger than a certain magnitude and in a certain time interval based on the known probability density function or distributions of the data used. The results showed that the log-normal distribution provides a significantly better fit to the recurrence time data than either the Gauss or the Weibull distribution.

Results of the prediction computations and corresponding probabilities for the ten year period (P_{10}) from 1992 to 2002 (based on the last event in the seismogenic source (1991 data) for magnitude Ms > 7.0) showed that the North and Central Kermadec segments exhibit high probabilities of P_{10} >0.5 and 0.59 respectively for the occurrence of a mainshock with Ms > 7.0 with an expected magnitude M_t of 7.6 and 7.4 respectively. The South Kermadec segment had a slightly lower P_{10} probability of ~ 0.37 with an expected magnitude of M_f ~ 7.2. Increasing the threshold to > 7.5 revealed that only seismogenic sources for North Kermadec can be computed; as there is no previous data for central and south Kermadec with magnitudes > 7.5. The computation results for the north Kermadec source define P_{10} of > 0.44 with expected maximum magnitude of M_f 8.0.

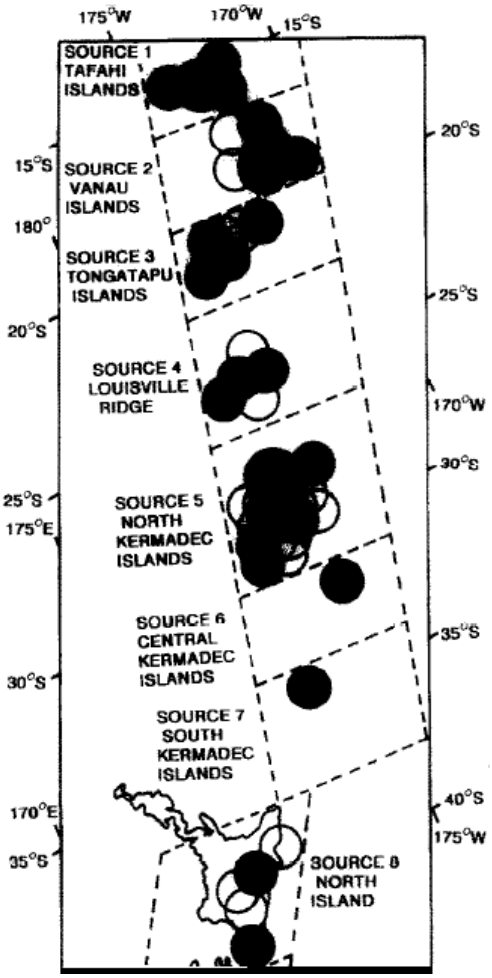

Figure 4.2-1 Three-seismogenic sources along the Kermadec arc follow the arc segmentation of Nishenko (1991). These are shown as North Kermadec (source 5), Central Kermadec (source 6), and South Kermadec (source 7) and are used to examine seismic activity along the Tonga-Kermadec Trench (source map: Papadimitriou, 1994).

Comparison of Papadimitriou (1994) predictions against the seismic record for the 10 yr period leading up to 2002 revealed the following events. Two earthquakes occurred at the boundary between the north and central Kermadec seismogenic regions in 1995 (Ms = 7.1) and 1997 (Ms = 7.0), and in 2001 (Ms = 7.1) near the northern end of the south Kermadec seismogenic region (at Rapuhia Scarp), even though this region has lower occurrence probabilities (P_{10}=0.37) when compared to the north (P_{10} = 0.5) and central

Kermadec (P_{10} = 0.59) regions. No data is available for central and south Kermadec seismogenic regions for events with magnitudes greater than 7.5, however north Kermadec and the Tonga-Vanau trench exhibit high P_{10} probabilities of 0.46 -0.53 for an expected magnitude M_s = 7.8-7.9 event. The highest expected magnitude for the north Kermadec region is 8.0 which has not occurred during this time period. Instead the Tonga-Vanau seismogenic region produced a magnitude Ms = 8.1 earthquake in 1995 (Table 4.2-1).

Table 4.2-1 Expected magnitude and probabilities for period 1993-2002 from Papadimitriou (1994) compared with actual events (1993-2010).

Seismogenic Source	**Expected magnitude and probabilities for period 1993 – 2002 (Papadimitriou, 1994)**				**Actual events for period 1993 – 2010**
	M_{min} > 7.0		**M_{min} > 7.5**		
	M_f	**P_{10}**	**M_f**	**P_{10}**	
Source 3: **Tongatapu Island**	7.6	0.79	7.9	0.46	**Ms = 8.1 (1995)** **Mw = 8.0 (2009)**
Source 4: **Louisville Ridge**	7.3	0.40	7.7	0.36	No event
Source 5: **North Kermadec Island**	7.6	0.50	8.0	0.44	**Ms = 7.1 (1995)**
Source 6: **Central Kermadec Island**	7.4	0.59	*No historical data	*No historical data	**Ms = 7.0 (1995)**
Source 7: **South Kermadec Island**	7.2	0.37	*No historical data	*No historical data	No event

* No probabilities were estimated for central and south Kermadec for the occurrence of a mainshock with Ms>7.5, since no earthquake with Ms>7.5 has occurred there during the time period covered by Papadimitriou 1994 data (1900-1992).

In 1995, a series of three earthquakes occurred along the Tonga-Kermadec Trench. Firstly at East Cape on February 5th, 1995 (Ms = 7.5), then Tonga (at the edge of Tonga Trench before it bends to the Northwest) on April 7th, 1995 (Ms = 8.1) and then in the middle of Kermadec Trench near Raoul Island on July 3rd at 29.21°S with a magnitude 7.1.

The long-term earthquake prediction of Papadimitriou (1994) shows that the central and southern part of the Kermadec seismogenic region has the potential to generate large shallow earthquakes with return periods greater than 170 years. However, as no historic record exists of large earthquakes along this particular seismogenic region one possibility is that two large seismic gaps exist (Bonnardot et al. 2007). Another possibility is aseismic motions are possibly common along this part of subduction zone (Pacheco et al., 1993). This was also identified by Ruff and Kanamori (1980) based on empirical correlation between the size of the largest earthquake in the zone and the convergence rate or age of the subducting plate. Ruff and Kanamori (1980) concluded that with a convergence rate of 6 cm/year and an age of 120 million years, the Kermadec subduction zone is relatively weakly coupled as reflected by the active back-arc opening occurring behind the Kermadec trench. Because of this they argue that a large component of aseismic slip is likely and therefore relatively few large to great shallow underthrusting earthquakes can be expected within the zone.

5.0 TSUNAMI FREQUENCY- MAGNITUDE ALONG THE KERMADEC TRENCH

5.1 Frequency – Magnitude from Historical and Paleo-tsunami data

The International Tsunami Database (ITDB/PAC2004) shows that 9 tsunamis have been generated within the Kermadec region since 1900 (see Figure 5.1.1). Two events occurred at the northern end of the Kermadec trench where the Louisville Ridge is being subducted, while another 7 events occurred in the northern segment.

Despite these 9 events, no reports of coastal damage were recorded for the east coast of New Zealand. De Lange and Healy (2001) and Goff et al. (2005) show that tsunami heights of less than 0.10 m were recorded at the Port of Auckland tide gauge for the 1976, 1977, 1982, 1986 and 1993 events. However, no data exists for events prior to 1976. Combining all tsunami records into a frequency-magnitude plot for the region suggests the occurrence of ~ 1 event in 12 years for small scale tsunami with wave heights <0.1 m. The probability of occurrence based on available tsunami historical records has been computed using ITDB/PAC2004 and is shown in Figure 5.1-2.

The historical data since 1900 does not show any large tsunamigenic earthquakes originating from the Kermadec subduction zone. However, as a general rule of thumb, large events within the subduction zone are likely to have return periods in the order of 200 to 1000 years, far exceeding the extent of the historic record.

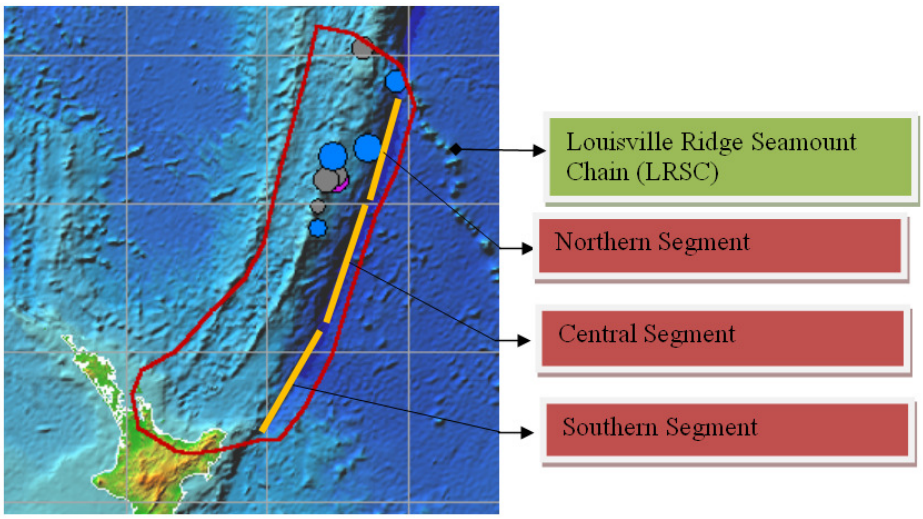

Figure 5.1-1 The spatial distribution of tsunamis in Kermadec region based on ITBD/PAC 2004 are confined to the area that extends from mid central segment to the north end of the Northern segment of Kermadec Trench, including the subduction point for the Louisville Ridge. No tsunamis have been generated along the southern segment of the Kermadec Trench.

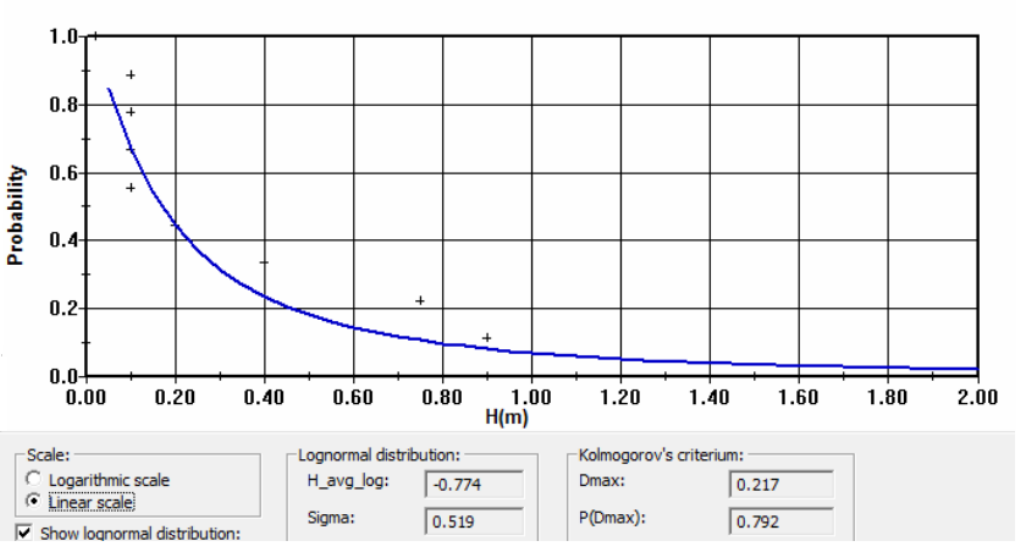

Figure 5.1-2 The occurrence probability of tsunami height based on available data (ITDB/PAC 2004, De Lange and Healy 2001 and Goff et al 2005) shows that tsunami with heights less than 0.2 m are common in this region.

Therefore paleotsunami records must be relied on to provide evidence of past inundation events that predate the NZ tsunami record. Goff et al (2010) showed that three large events occurred (6500 year BP, 2800 year BP and in 1450 AD) as shown in Figure 5.1-3. The authors considered that the first two events were likely to be sourced from the Tonga-Kermadec Trench, with the last event originating from an eruption of the Kuwae Volcano (Vanuatu) in 1453/53 AD.

However, considering the massive and continuous distribution of tsunami deposits along the east coast and northwest coast of North Island and the dispersive nature of volcanogenic tsunami (even though it is larger than the Tambora caldera ~ 12 km x 6 km), the Kuwae source for this third event is at best questionable and a Kermadec source is considered more likely. Prasetya (1998), De Lange and Prasetya (1999), Prasetya et al (2000 and 2008), showed that the volcanogenic tsunamis are only devastating locally and or where eruptions occur within semi-enclosed seas or straits (Krakatau 1883, Tambora 1815 and Banda Api 1600, Mt Healy and White Island scenarios). The tsunamis generated from these sources may propagate for long distances but their amplitudes decrease rapidly due to a dispersive character of the tsunamis generated by the volcanic activities (Mehaute and Wang, 1996, De Lange and Prasetya, 1999 and De Lange et al. 2001).

In summary (Table 5.1-1), the historic and paleo-tsunami data indicates the occurrence of 13 events over a 6800 year period (1 in 523 years). Small events with tsunami height <0.1 m (recorded at the Auckland Port) or < 0.5 m outside the Hauraki Gulf (Bay of Plenty and Eastern Coromandel) represent a frequency of 1 event every 10 years (10 events in 110 years). Large event with tsunami heights <10 m have an average occurrence interval of 1 in 2267 years based on 3 events over 6800 years. Goff et al (2005) previously suggested an occurrence interval of 1 in 1300 years for large events based on 2 events in 2600 years.

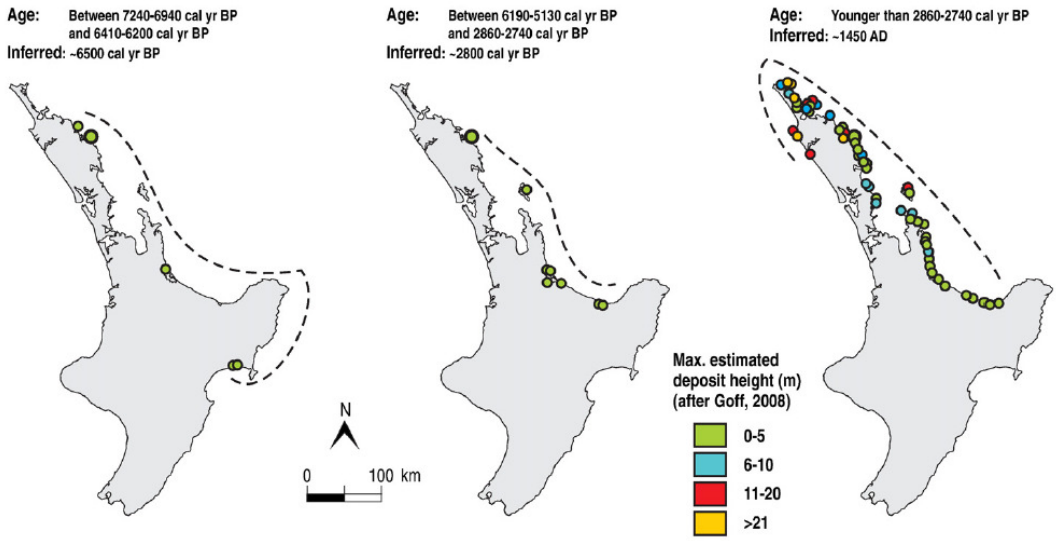

Figure 5.1-3 Paleotsunami data along the coast of the North Island based on Goff et al. (2010) shows three large events with tsunami run-up heights ranging from 5 to 20 m, with some areas exceeding 21 m. The event in 6800 was potentially generated by a large earthquake that ruptured both the Hikurangi and Kermadec Trench. Wallace et al.2009 indicated that lesson from the 2004 Sumatra event lead to a possibility of more serious scenario that involve simultaneous rupture of the entire Hikurangi-Kermadec Trench (with similar scale of ~ 1500 km rupture length). The event in 2800 is likely to have been generated by a rupture of the South and Central Kermadec Trench, while the 1450 AD event involved the whole Kermadec Trench with extension into the Tonga Trench.

Table 5.1-1 Summary of tsunami frequency-magnitude from Kermadec region

	DATA SOURCES	DATE	Tsunami Height (m) – New Zealand coast
1	ITDB/PAC2004	1 May 1917, Ms = 7.9, depth = 60 km	unknown
2	ITDB/PAC2004	16 November 1917, Ms = 7.5 km, depth = 60 km.	unknown
3	ITDB/PAC2004	31 March 1963, Ms = 7.2 , depth = 39 km	unknown
4	ITDB/PAC2004	25 July 1968, Ms = 7.0, depth 66 km	unknown
5	ITDB/PAC2004,	14 January 1976 (couplet), Ms = 7.8, depth = 69 km	unknown
6	ITDB/PAC2004, De Lange and Healy (2001), Goff et al (2005)	14 January 1976 (couplet), Ms = 8.2, depth = 33 km	< 0.1 m at Auckland Port
7	De Lange and Healy (2001), Goff et al (2005)	22 June 1977,	<0.1 m at Auckland Port
8	ITDB/PAC2004	10 October 1977, Ms = 7.2, depth = 33 km.	unknown
9	De Lange and Healy (2001), Goff et al (2005)	19 December 1982,	<0.1 at Auckland Port
10	ITDB/PAC 2004, De Lange and Healy (2001), Goff et al (2005)	20 October 1986, Ms = 8.3, depth = 29 km	< 0.1 at Auckland Port
11	Goff et al. 2005 (2010)	Early 15th C (1450 AD)	5 to 21 m
12	Goff et al. 2005 (2010)	2500-2600 (2800 cal yr BP)	0 - 5m
13	Goff et al. 2005 (2010)	6800 cal yr BP	0 – 5 m

SUMMARY

13 events in 6800 years (1 in 523 years)

Small events

10 in 110 years (1 in 10 years)

Large events

3 in 6800 years (1 in 2267 years)

5.2 Frequency – Magnitude using McCaffrey 2008 method and Abe (1995)

Combining the seismic gap concept (McCann et al., 1979), with the length over which the fault system extends continuously along a convergent plate boundary (Okal and Synolakis, 2008) and basin boundaries, allows potential tsunamigenic earthquake events to be estimated using the methods of McCaffrey (2008). Strong variability and unpredictability around rupture fragmentation during major earthquakes along the subduction zone (as indicated by Okal and Synolakis (2008)) also needs to be taken into account.

McCaffrey (2008) estimated the maximum earthquake magnitude (the seismic moment of M_o^{max}) from the longest possible subduction zone rupture length (L) as

$$M_o^{max} = \mu\, u_{av}\, L\, Z_{max} / \sin\delta,$$

where μ is the shear modulus, Z_{max} is the maximum depth of dip (in metre), δ is the average fault dip angle derived from earthquake mechanism (in degree), and u_{av} is the average slip in the earthquake which is estimated from the rupture length (in metres) by

$$u_{av} \sim 2.5 \times 10^{-5} L,$$

with the corrected factor of 0.2 to 0.5 as fault width corrections.

Finally, the maximum moment magnitude (M_w^{max}) is estimated from the seismic moment using equation

$$M_w^{max} = 2/3 \log Mo - 6.07, \text{ Mo in Nm.}$$

The recurrence time for large events can be estimated from the relationships

$$T = u_{av}/f\chi\nu,$$

where ν is the plate motion rate, f is the fraction of the total seismic moment represented by large earthquakes and χ is the fraction of slip on the boundary that occurs seismically. For large earthquakes the sum of f and χ is equal to 1 with f varied from 0.32 to 0.45 for the subduction zone (McCaffrey, 2008).

An estimation of maximum fault rupture length is made first (Figure 5.2-1) based on combination of seismic gaps identified previously in Figures 4.1-2a and 5.1-1 as well as possible fault rupture of the whole Kermadec and Hikurangi Trench (Wallace et al., 2009). The fault segment arrangements and combination for the computation are shown in Figure 5.2-2 with results in Table 5.1 and 2 (Appendix 1).

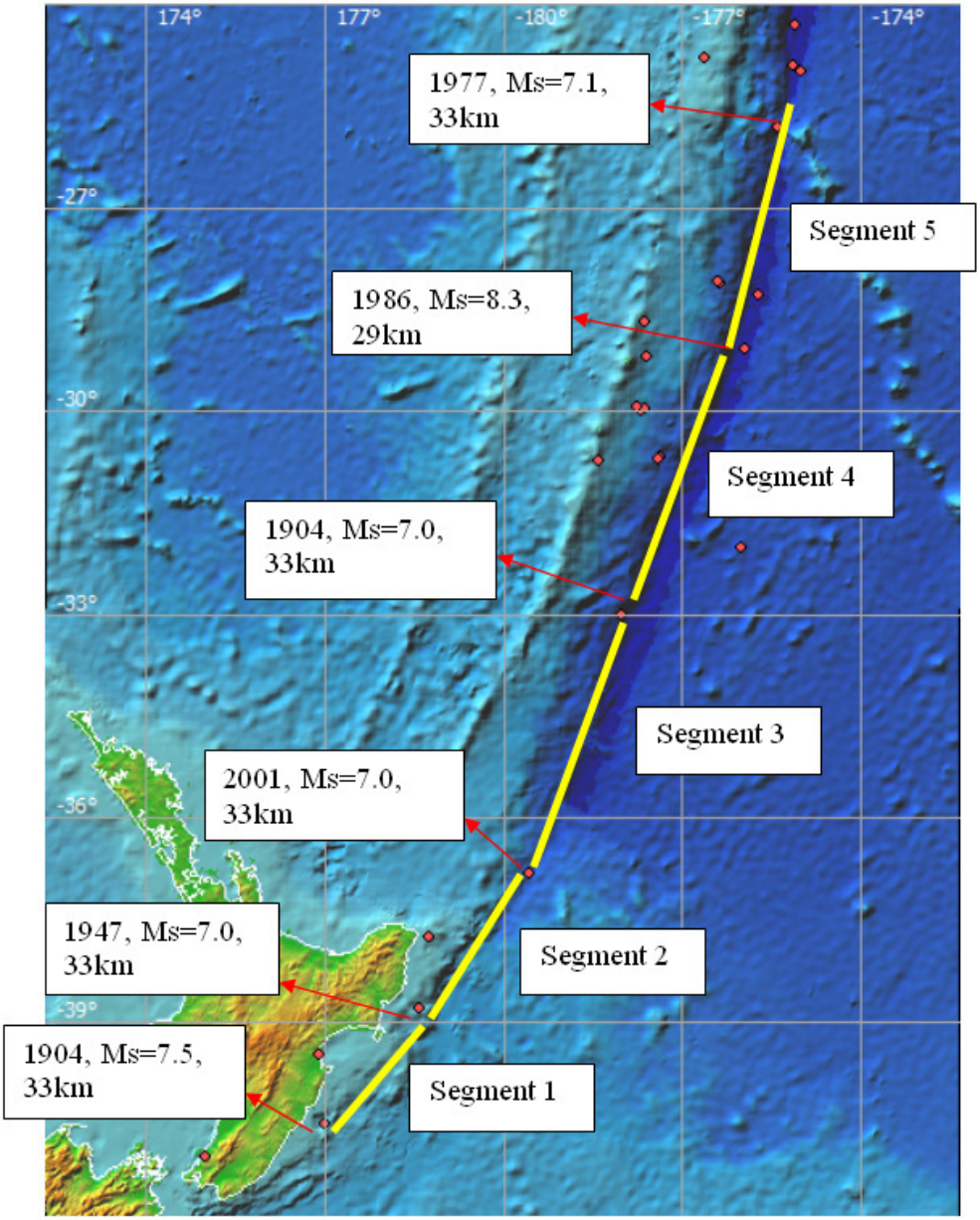

Figure 5.2-1 The fault segments along the Hikurangi – Kermadec Trench derived from seismic gap analysis of large earthquakes ≥ Ms 7.0.

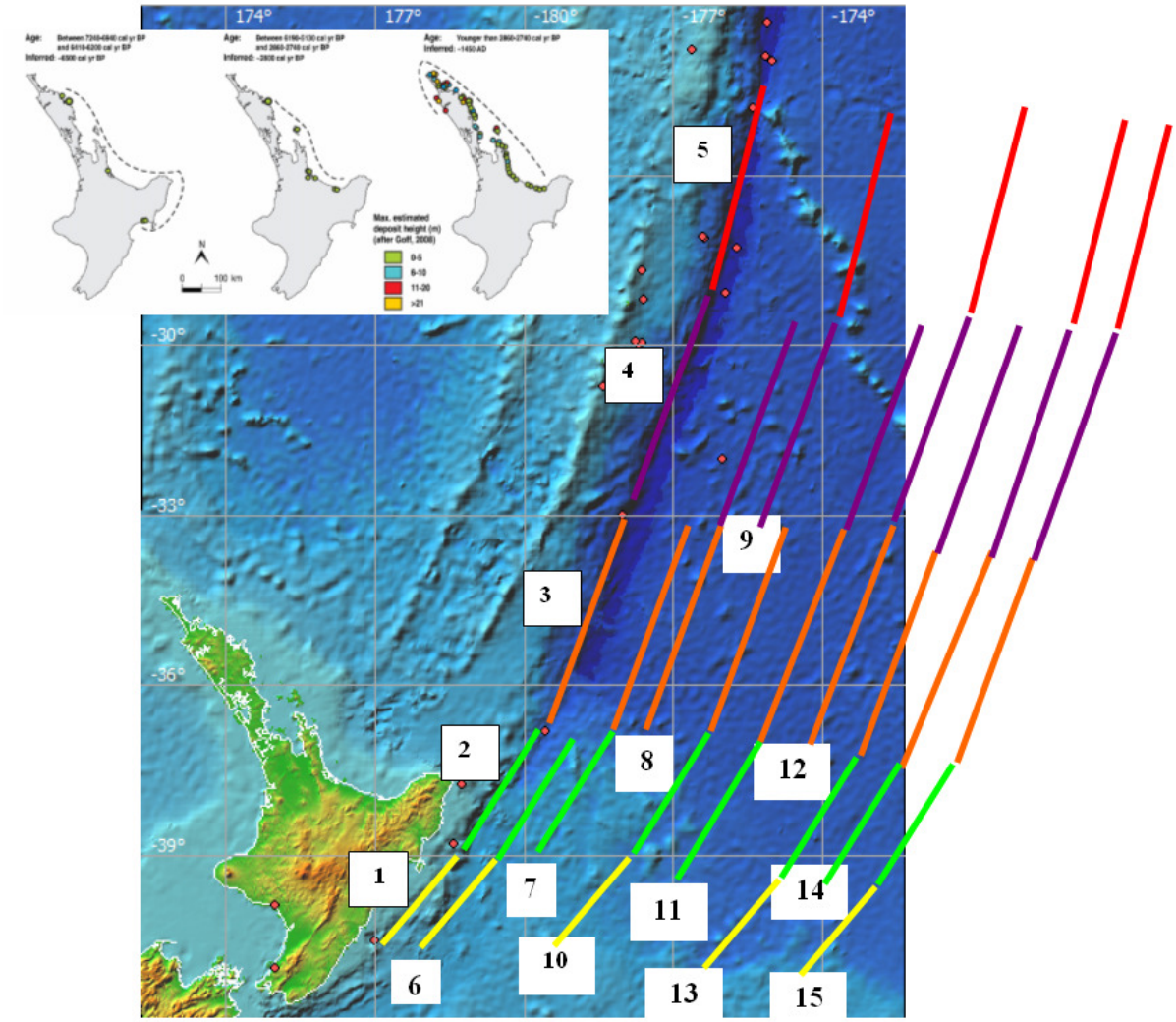

Figure 5.2-2 The fault segments along the Hikurangi – Kermadec Trench arrangements and combinations for the frequency-magnitude assessment based on McCaffrey 2008 and Abe 1985 method.

Abe (1995) provides an empirical formula as predictive equations to estimate tsunami heights from the earthquake magnitude. The empirical equations are:

$$\text{Log } H_e = 0.5\ Mw - 3.30 + C \qquad \text{for } R < Ro \qquad (1)$$

$$\text{Log } H_e = Mw - \log R - 5.5 + C \qquad \text{for } R > Ro \qquad (2)$$

H_e is the estimated tsunami height (peak to trough) in metres, R is the distance from the epicentre in km. The value of the constant C, is C=0.2 for tsunami generation in a backarc setting and C=0 for a forearc setting, Mw is the earthquake moment magnitude. If the moment magnitude is not determined, then the surface-wave magnitude (Ms) can be used. Surface-wave magnitudes must be used with caution because the Ms scale saturates and can significantly underestimates earthquake energy for earthquakes greater than about

Mw 8.5. Ro is taken as the radius (km) of a circular generation area having an area equivalent to the expected deformed region produced by the earthquake, and is given by:

$$\text{Log } Ro = 0.5Mw - 2.25 \quad (3)$$

These equations allow the calculation of tsunami wave height (peak to trough) along the eastern Coromandel coast, However, the empirical relations established by Abe (1995) should be used with caution as they tend to over-predict local maximum wave height (near the source) within a factor of 1.5 and in some cases 2 -4 times larger than the numerical models (Chick et al., 2001).

Using those Abe (1995) formulas, the tsunami wave height (peak to trough) of the eastern Coromandel Peninsula are calculated with earthquake magnitude derived from the method of McCaffrey (2008) (Table 4). The results also can be seen in Table 4. For the individual segment ruptures (segments 1, 2, 3, 4, and 5), the highest tsunami height at the eastern Coromandel Peninsula is produced by:

- segment 3 (Mw = 8.4 - 8.62) with height of 2.24 - 3.71 m, follow by
- segment 2 (Mw = 8.14 - 8.34) with tsunami height 1.84 m - 2.93 m, and
- segment 4 (Mw = 8.71) with tsunami height 1.72 m - 2.73 m

Combinations of segments ruptures show the important of segment 3 in producing the highest tsunami height at the eastern Coromandel Peninsula. Increasing the earthquake magnitude without involving segment 3 generates a smaller tsunami. A combination of segment 1 and 2 (Mw = 8.68), and segment 4 and 5 (8.99) provides maximum tsunami height of 6.5 m and 5.2 m respectively. While a combination of segment 2 and 3 (Mw = 8.9), and 3 and 4 (Mw = 9.07) provides the highest tsunami height of 10.67m and 10.32 m respectively.

Further combination of segment rupture (more than two segment involve ~ Mw > 8.5) provides a significant tsunami wave height to the eastern Coromandel Peninsula, with tsunami wave height varies from 5.2 m to 18.9 m (Mw = 9.4) for computation without rupture width corrections, and from 4.1 m to 11.9 (Mw = 9.2) for computation with rupture width corrections (Table 4).

The trends of maximum tsunami height from this study are similar with the previous studies done by NIWA where the eastern Coromandel was significantly affected by tsunami from the source along the southern and middle of the Kermadec Trench.

Using the McCaffrey (2008) method, we calculate earthquake magnitudes from segments along the Hikurangi and Kermadec Trench to be range between 8.2 and 9.4; results that are in agreement with those of Wallace et al. (2009). The calculated return periods varied from 102 to 892 years with tsunami height at the coast based on Abe (1995) formula varying from 1 to 19 m.

Computation results (Table 5.2 – Appendix 1) using McCaffrey (2008) and Abe (1985) formulae indicate that for individual segments, a rupture occurring along segment 3 generates the highest tsunami wave (3.71 m) at the eastern Coromandel coast while the

smallest tsunami height is produced by a rupture along segment 5 (the northern end of Kermadec Trench). For segment combination scenarios, the largest tsunami height results from a rupture of all five segments, while the smallest is produced by a source combination of segments 1 and 2 of the Hikurangi Trench. A summary of earthquake magnitude, return periods and estimate tsunami heights at the coast can be seen in Table 5. The tsunami height at the coast for the 'all' segment rupture scenario fits with paleotsunami data from Goff et al (2010) in particular the 1450 AD event. However, there is a big difference in the return period for this event compared to the return period calculated from the paleotsunami data.

5.3 The magnitude-frequency parameters for Kermadec Trench of Power et al (2011).

Power et al (2011) assess the tsunami hazard posed to New Zealand by the Kermadec Trench. A set of scenarios for large earthquakes were developed based on reviewed data on the larger historical earthquakes that have occurred and plate kinematic and fault-locking results from block modelling of earthquake slip vector data and GPS velocities. Based on this assessment, the Kermadec Trench is divided into three segments, namely segment A, B, and C that are similar to the southern, central and northern end segments of the previous works (Goff et al.2006, DeLange et al 2008) and correspond to segments 3, 4 and 5 (Figure 5.3-1) of this study. Four scenarios are proposed: a single event that involves individual segments and the whole rupture of segments A, B, and C. Based on fault parameters of each segment this corresponds to events with magnitudes Mw = 8.5 (segment A), Mw = 8.9 (segment B), Mw = 8.8 (segment C), and Mw = 9.4 (segment A+B+C) (Table 5.3-1). This last event scenario is comparable to the 2004 Sumatra earthquake. Their results demonstrate that the Coromandel regions had a significant threat if a large earthquake (Mw >~8.5) occurs on the southern (segment A) or middle regions (segment B) of the Kermadec Trench and the combine segment ruptures (the entire segment of the Kermadec Trench~ Segment A+B+C).

Power et al. (2011), proposed logic trees for the magnitude-frequency parameters of large earthquakes originating from this trench, which are intended to form the basis for future probabilistic studies. The event scenario that involves the whole rupture of segment A, B and C in the logic tree is unlikely to ever occur as only 12% weighting was assigned to magnitude frequency distribution that permits rupture as large as Mw 9.4 (Power et al.2011). However, Power et al (2011) include this scenario as the possibility of rupture of the entire trench can not be ruled out empirically (McCaffrey, 2007), and also the fact that the Sumatra earthquake – Indian Ocean Tsunamis that involved a more than 1250 km length of fault ruptures with magnitude ~ Mw = 9.2 occurred at the place that was thought impossible to generate such a large earthquake (McCaffrey, 2008). Furthermore, recent paleo-tsunami studies along the North Island New Zealand (Goff et al. 2010) show the evidence of continuous spread of tsunami deposit in ~AD1450's along the North Island which is matched with the tsunami height distribution pattern from tsunami generated by the scenario events that involving the whole rupture of Kermadec Trench (Goff et al.2006, De Lange et al. 2008, Prasetya et al. 2008).

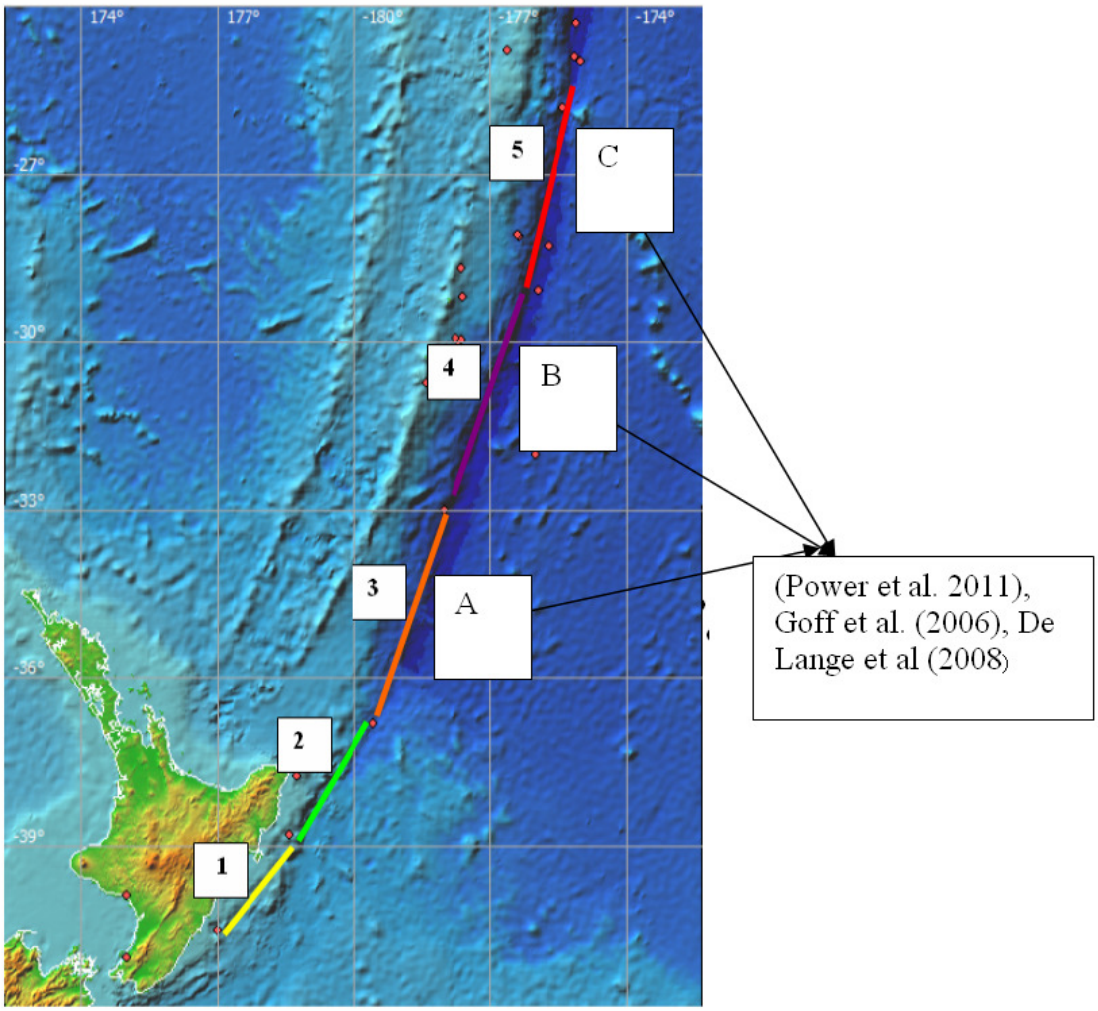

Figure 5.3-1 Numbers 1,2,3,4 and 5 are segmentation based on all previous studies on the region which are incorporated into the recent study (in completion). The EQC-FRST recent research done by Power et al (2011) concentrated on three segments (3, 4, and 5) or they called segment A, B, and C.

Table 5.3-1 Fault parameter of Kermadec Trench (Power et al.2011).

Segment	Length	Width	Slip	Magnitude
A	300 km	100 km	5.0 m	Mw 8.5
B	600 km	100 km	10.0 m	Mw 8.9
C	500 km	100 km	8.0 m	Mw 8.8
A+B+C	1400 km	100 km	22.0 m	Mw 9.4

6.0 NUMERICAL MODELLING

A numerical modelling assessment is carried out using the COMCOT tsunami modelling code (Wang, 2010). The grid resolution for this numerical modelling assessment is based on GEBCO 08 3 arc second and SRTM 30 arc second for the topography data. This regional modelling grid setup is as follow (Figure 6.0 -1):

Level 1: Grid resolution of 1 arc minutes (~ 1.8 km)

Level 2: Grid resolution of 0.2 arc minutes (~360 m)

Level 3: Grid resolution of 0.05 arc minutes (~90 m)

Level 4: Grid resolution of 0.025 arc minutes (~45 m)

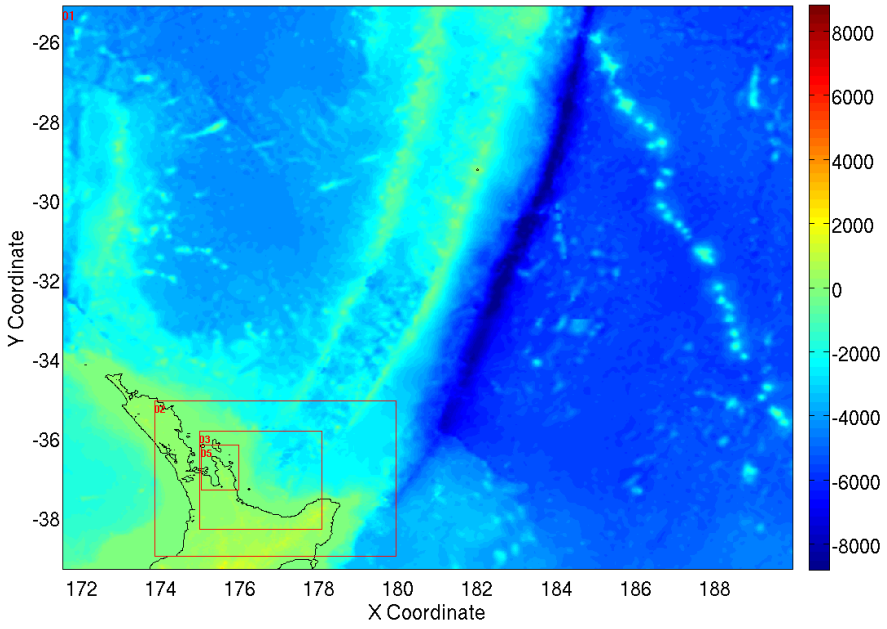

Figure 6.0-1 The nested grid arrangement for numerical modelling assessments (data source: Gebco08 3 arc second, and SRTM 30 arc second resolution).

6.1 Numerical modelling of combination segment 2, 3, 4 and 5 based on McCaffrey (2008) fault parameters

As mentioned in section 5, an empirical approach using McCaffrey (2008) and Abe formula (1995) show the eastern Coromandel Peninsula is mostly affected by tsunamis generated from segment 2, 3 and 4 or greater events that involving a combination of segment 2, 3, and 4. The tsunami wave height ranges from 2.0 to 4.0 m for individual segments and ranges between 9.0 m to 12.0 m for larger events with segment combinations (2, 3, 4 and 5) or the whole Kermadec segment to the north of Hikurangi segments (Figure 5.3-1).

A numerical modelling assessment using COMCOT tsunami model (Wang, 2010) is carried out for large events that involve a combination of segment 2, 3, and 4 (Mw = 9.1) with applying the width correction factor of 0.67. The fault parameters used on this model are based on McCaffrey (2008) as follow (Table 5.1 and 2 Appendix 1): fault length: 1237 km (segment 2, 3 and 4); width: 100 km, slip/vertical deformation = 20.0 m; depth = 5 km; dip angle = 16°; Slip angle = 90°; strike = 209° - 210°. The general distribution of the tsunami from the source is illustrated in Figure 6.1-1. The sub-regional model result shows the maximum tsunami elevation that occurs along the east coast of eastern Coromandel Peninsula and Waikato Region between 5.5 to 10 m (Abe (1995) formula provide a maximum tsunami wave height of 9.39 m). And an inundation occurs towards Firth of Thames low-lying areas with tsunami elevation above MSL ~ 1 – 2.5 m.

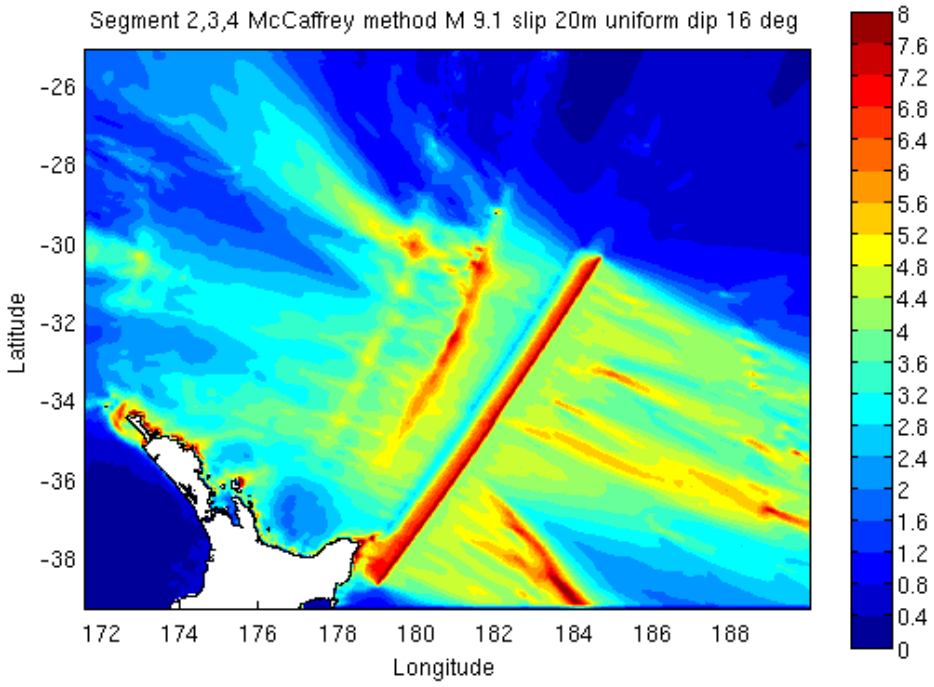

Figure 6.1-1 The maximum tsunami elevation distribution from the segment 2, 3, 4 sources. Scale bar unit is in metres.

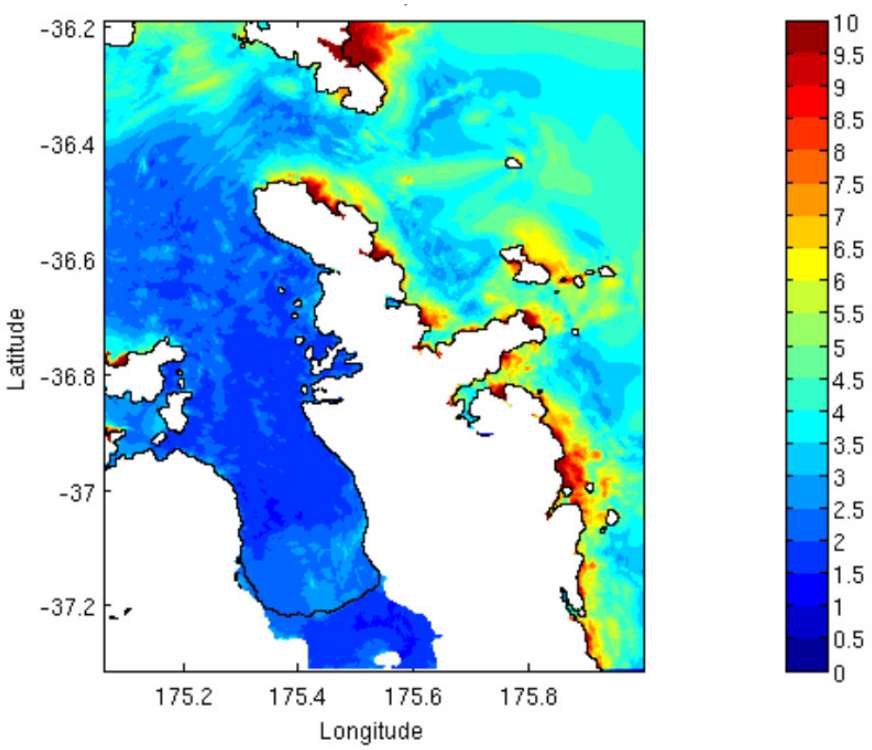

Figure 6.1-2 The maximum tsunami elevation that occurs along the east coast of eastern Coromandel Peninsula between 5.5 to 10 m (Abe (1995) formula provide a maximum tsunami wave height of 9.39 m). The model results also show that an inundation occurs towards Firth of Thames low-lying areas with tsunami elevation above MSL ~ 1 – 2.5 m. Scale bar unit is in metres.

6.2 Numerical Modelling of Power et al (2011) faults parameters

6.2.1 Scenario from Segment A

An earthquake with magnitude of Mw 8.5 was assigned for segment A located at the southern end of Kermadec trench with general fault parameters as shown in Table 6.2.1-1. In modelling this event scenario, the source area is divided into 6 unit sources (100 km x 50 km) with dip angles varies from 4^o to 11^o, strike angles from 202^o to 212^o, and depth from 4 km to 10 km. The slip angles is uniform 90^o and slip = 5.0 m. The regional maximum tsunami elevation from this source is shown in Figure 6.2.1-1. Tsunami were affected most of the east coast of North Island from the East Cape towards the northern end of North Island. The sub-regional model for Waikato Region shows that the maximum tsunami elevation above MSL along the east coast varies from 1.5 m to 3.5 m with the maximum elevation occurs in most of Bays and estuaries. The model is run at the Mean High Water Spring condition.

Table 6.2.1-1 General fault parameters for Segment A

Segment	Length	Width	Slip	Magnitude
A	300 km	100 km	5.0 m	Mw 8.5

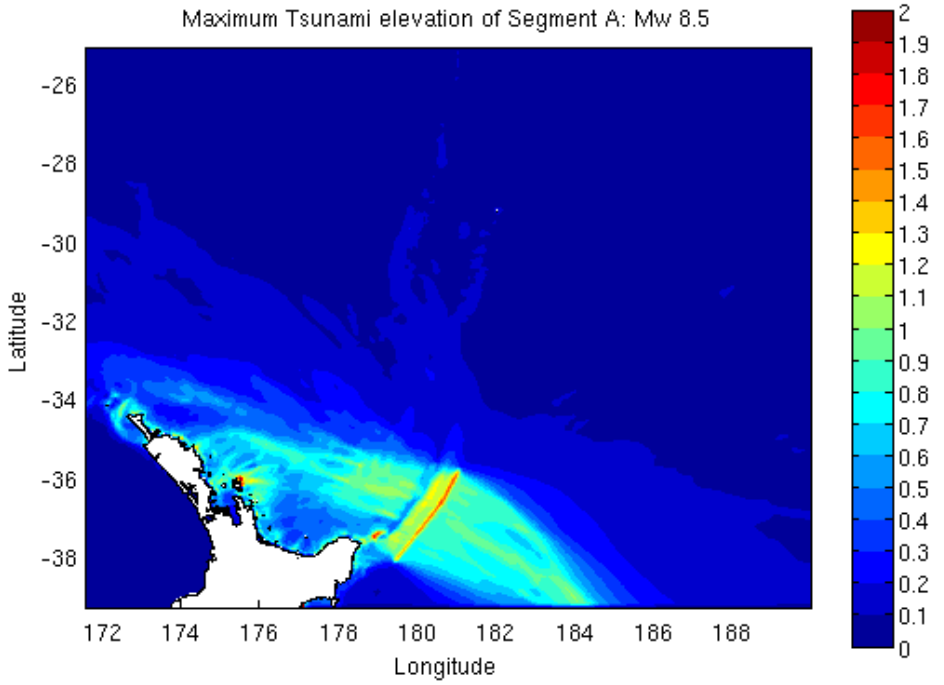

Figure 6.2.1-1 The maximum tsunami elevation above MSL from segment A. Scale bar unit is in metres.

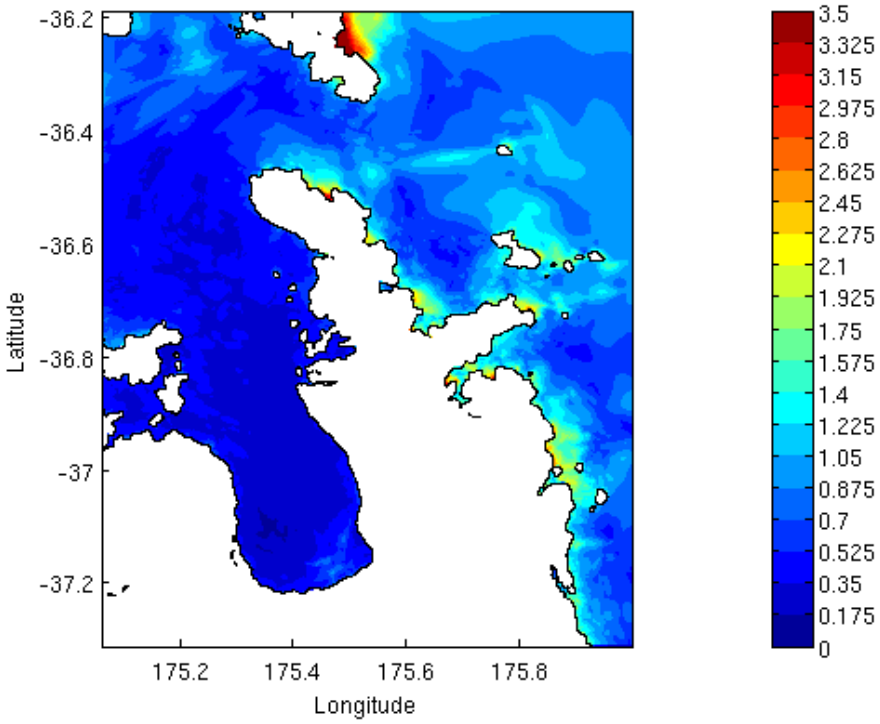

Figure 6.2.1-2 The maximum tsunami elevation above MSL from segment A for Waikato Region. Scale bar unit is in metres.

6.2.2 Scenario from Segment B

An earthquake with magnitude of Mw 8.9 was assigned for segment B which is located in the middle of Kermadec Trench, with fault parameters shown in Table 6.2.2-1. In modelling this event scenario, the source area is divided into 12 unit sources (100 km x 50 km) with dip angles varies from 5° to 17°, strike angles from 197° to 205°, and depth from 6 km to 16 km. The slip angles is uniform 90° and slip = 10.0 m. The regional maximum tsunami elevation from this source is shown in Figure 6.2.2-1. Tsunami were affected most of the east coast of North Island from the East Cape towards the northern end of North Island. The sub-regional model for Waikato Region shows that the maximum tsunami elevation above MSL along the east coast varies from 1.5 m to 3.5 m with the maximum elevation occurring only inside the Port Charles, Waikawau and Little Bay. The model is run at the Mean High Water Spring condition.

Table 6.2.2-1 General fault parameters for Segment B.

Segment	Length	Width	Slip	Magnitude
B	600 km	100 km	10.0 m	Mw 8.9

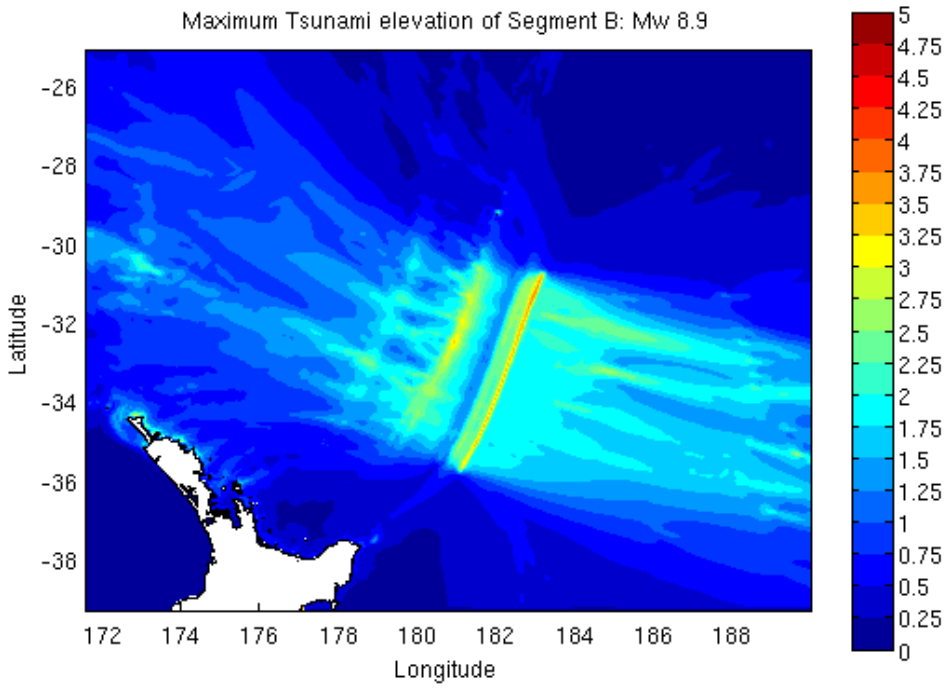

Figure 6.2.2-1 The maximum tsunami elevation above MSL from segment B. Scale bar unit is in metres.

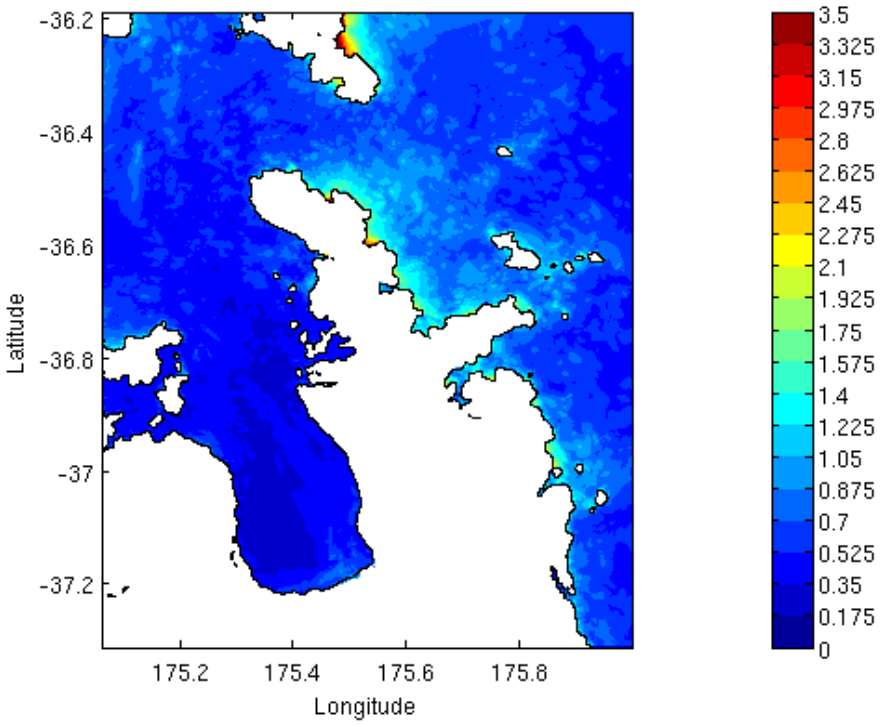

Figure 6.2.2-2 The maximum tsunami elevation above MSL from segment B for Waikato Region with maximum elevation only occurs to Port Charles, Waikawau, Little Bays and Great Mercury Island. Scale bar unit is in metres.

6.2.3 Scenario from Segment C

An earthquake with magnitude of Mw 8.8 was assigned for segment C (Power et al. 2011) which is located at the northern-end of the Kermadec Trench. General fault parameters are shown in Table 6.2.3-1. In modelling this event scenario, the source area is divided into 10 unit sources (100 km x 50 km) with dip angles varies from 9° to 17°, strike angles from 190° to 202°, and depth from 6 km to 20 km. The slip angles is uniform 90° and slip = 8.0 m. The regional maximum tsunami elevation from this source is shown in Figure 6.2.3-1 where most of the energy from the tsunami is not directed towards New Zealand. The sub-regional model for Waikato Region shows that the maximum tsunami elevation above MSL along the east coast varies from 0.5 m to 1.0 m. The model is run at the Mean High Water Spring condition.

Table 6.2.3-1 General fault parameters for Segment C.

Segment	Length	Width	Slip	Magnitude
C	500 km	100 km	8.0 m	Mw 8.8

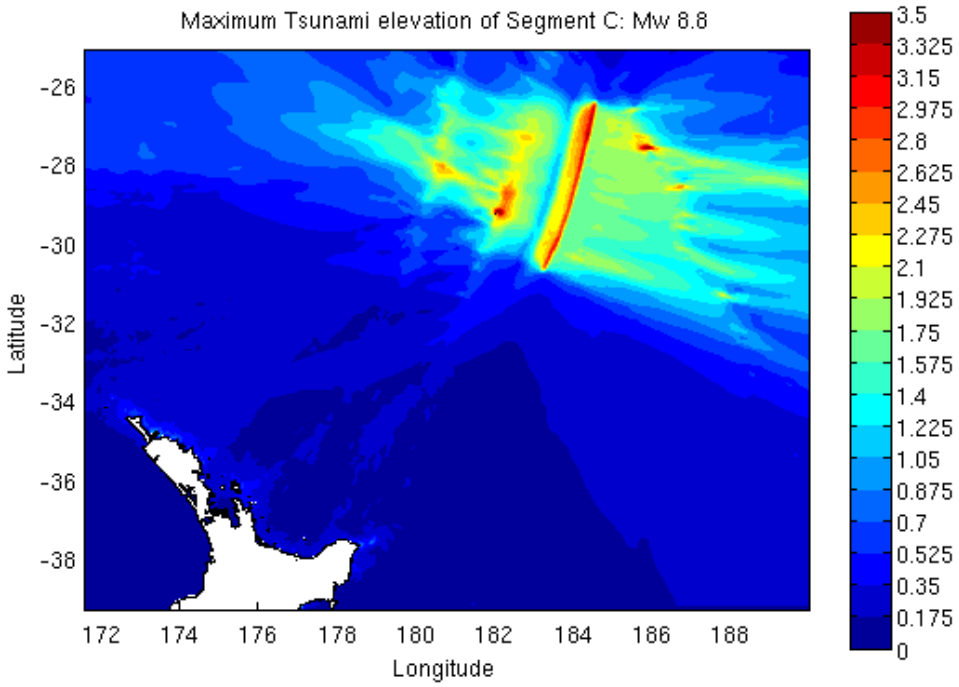

Figure 6.2.3-1 The maximum tsunami elevation above MSL from segment C at the northern-end of the Kermadec Trench in which most tsunami energy is not directed towards New Zealand. Scale bar unit is in metres.

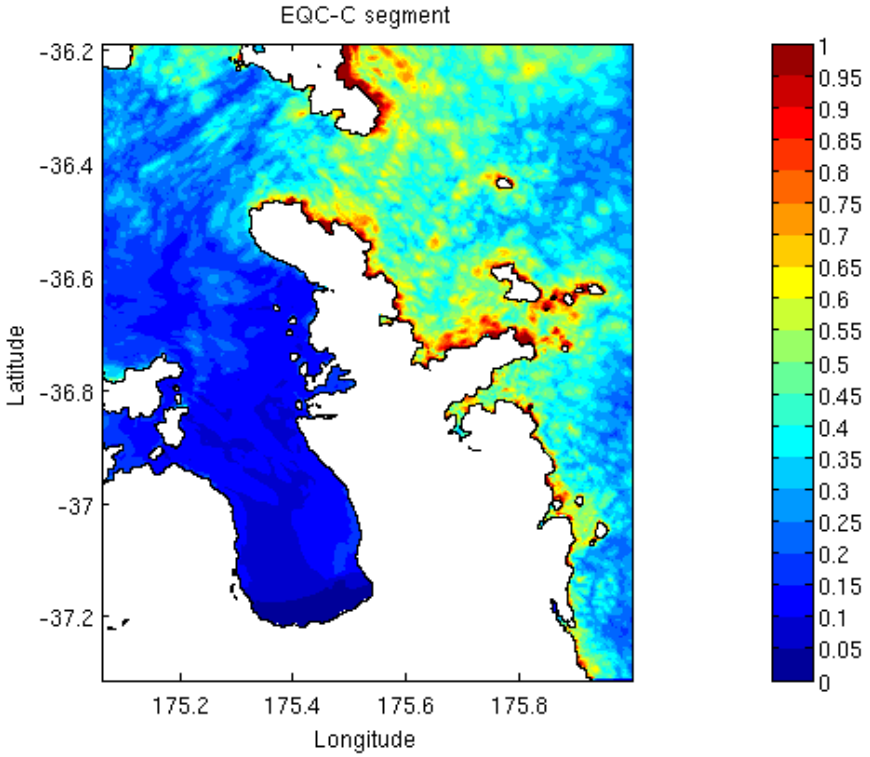

Figure 6.2.3-2 The maximum tsunami elevation above MSL from segment C for Waikato Region that varies from 0.5 m to 1.0 m. Scale bar unit is in metres.

6.2.4 Scenario from Combine Segment A, B, C (the entire segment ruptures)

An earthquake with magnitude of Mw 9.4 was assigned by assuming that the entire subduction zone (segment A, B, and C) is ruptured (Power et al. 2011). General fault parameters are shown in Table 6.2.4-1. In modelling this event scenario, the source area is divided into 28 unit sources (100 km x 50 km) with dip angles varies from 4° to 17°, strike angles from 190° to 205°, and depth from 4 km to 20 km. The slip angles is uniform 90° and slip values is uniform 22.0 m. The regional maximum tsunami elevation from this source is shown in Figure 6.2.4-1. The east cost of North Island of New Zealand is affected by tsunamis originating from segments A and B. The sub-regional model for Waikato Region shows that the maximum tsunami elevation above MSL along the east coast varies from 5.0 m to 8.0 m. The model is run at the Mean High Water Spring condition.

Table 6.2.4-1 General fault parameters for Segments A, B and C.

Segment	Length	Width	Slip	Magnitude
A+B+C	1400 km	100 km	22.0 m	Mw 9.4

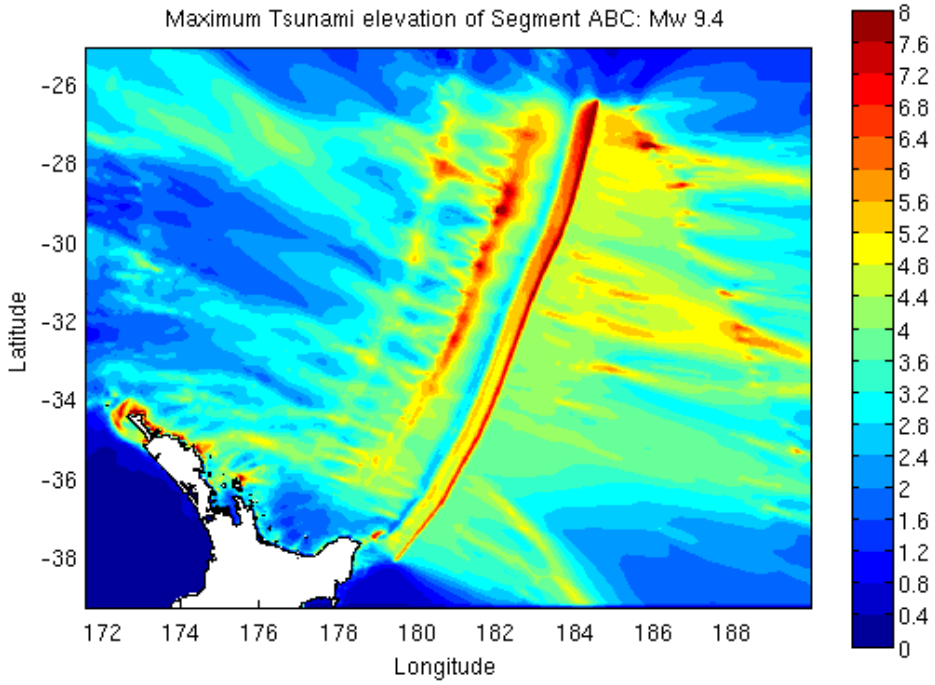

Figure 6.2.4-1 The maximum tsunami elevation above MSL for the scenario in which the entire ruptures of segments A, B and C rupture shows most of tsunami impacted to the east coast of New Zealand are originated along the segment A and B. Scale bar unit is in metres.

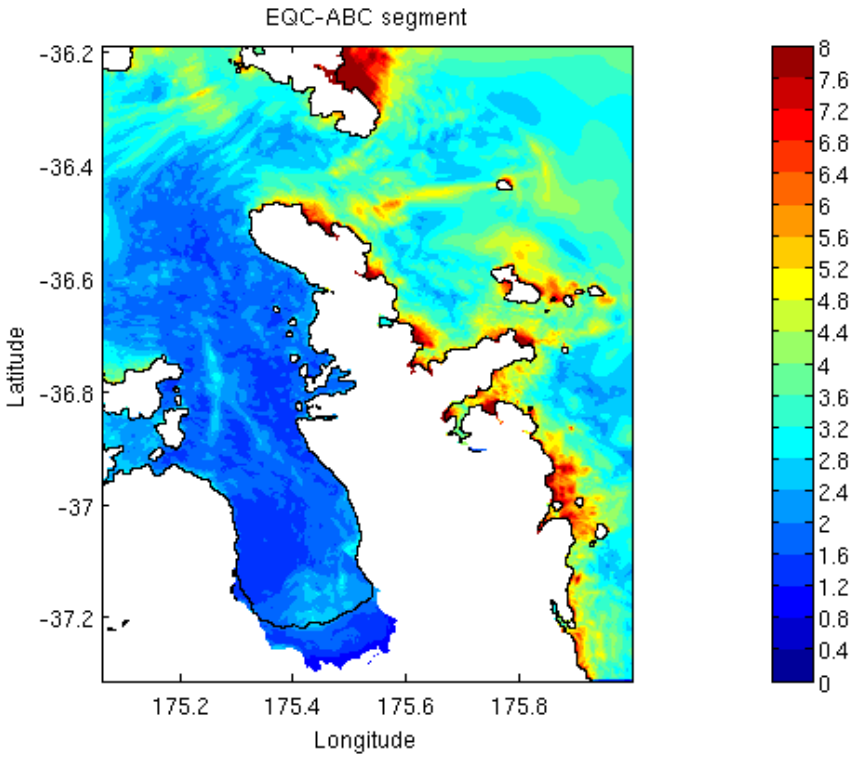

Figure 6.2.4-2 The maximum tsunami elevation above MSL along the Waikato Region varies from 5.0 m to 8.0 m and inundation occurs at the Firth of Thames with tsunami elevation ~ 0.5 m to 2.5 m above MSL. Scale bar unit is in metres.

6.3 Numerical Modelling of Local Sources from Bay of Plenty Region.

Local faults described by Lamarche and Barnes (2005) were used by Walters et al. (2006) in assessing the tsunami impact from local sources within the Bay of Plenty region. These local faults are a composite Astrolabe fault (AST-C1), Volkner fault (VOLC-C1) and White Island fault (WIF-C1) and primarily normal faults in the offshore of Taupo Volcanic Zone. Normal faulting in this area rarely exceeds 2 m single event vertical displacement, but with the larger boundary faults may be capable of larger seabed displacements (Walter et al. 2006). Lamarche and Barnes (2005) indicated that a typical return period for these faults vary from few hundred to 1000's of years.

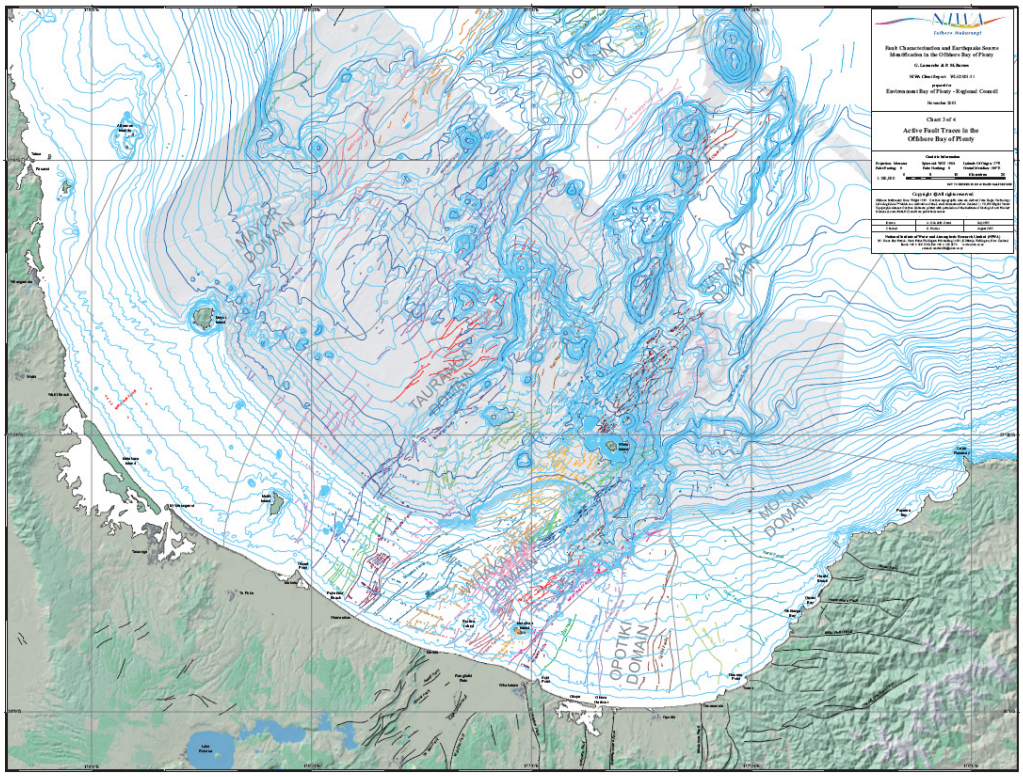

Figure 6.3-1 Fault distribution and earthquake source identification in the offshore of Bay of Plenty overlay with the multibeam bathymetry survey data (source: Lamarche and Barnes, 2005).

Walter et al (2006) based on Lamarche and Barnes (2005) delineates these three composite faults as illustrated in Figure 6.3-2. The composite Astrolabe faults to the west side Bay of Plenty region with 17.65°NE alignment (AST-C1), the composite Volkner faults in the middle (VOLC_C1) with 25.49°NE alignment and the White Island faults (WIF-C1) to the east with 36.79°NE alignment.

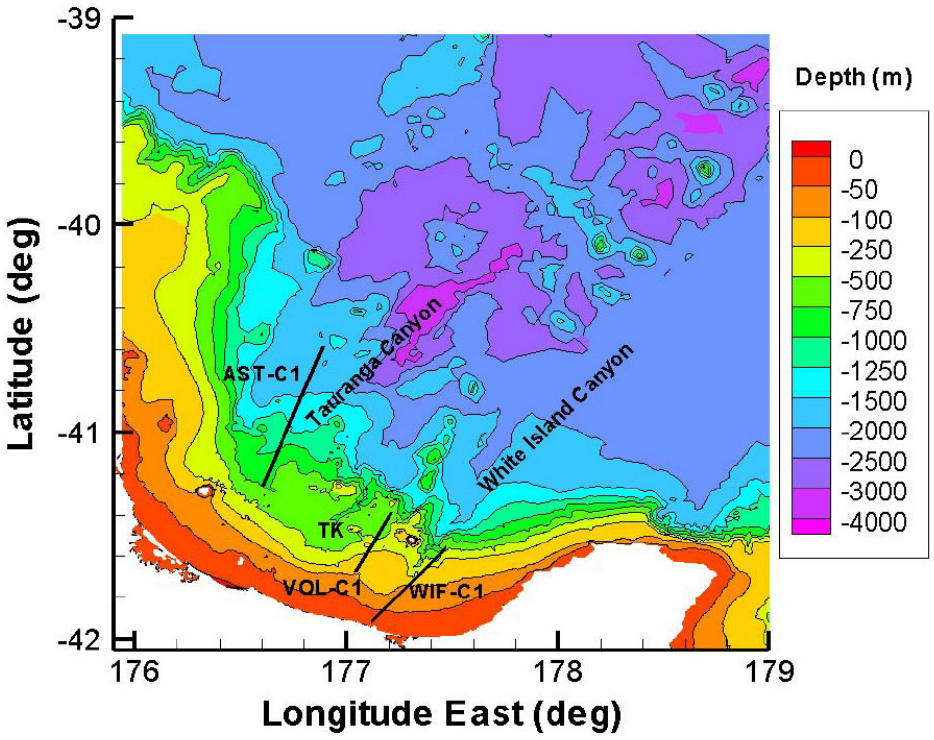

Figure 6.3-2 Fault delineation based on Lamarche and Barnes (2005) in the offshore of Bay of Plenty (Walter et al. 2006) is being used in assessing the potential tsunami impact to the Waikato region on this study.

A numerical modelling of tsunami generation, propagation and inundation at regional scale from these sources towards the east coast of Waikato region is carried out. Fault parameters from each faults is derived from Lamarche and Barnes (2005). The grid resolution of this regional model are derived from Gebco 08 (30 arc-second resolution) with grid resolution of 0.1667 arc-minute (~ 300m) for the model setup including the generation region and 0.0556 arc-minute (~ 100m) for the areas that cover the Waikato region.

6.3.1 A composite Astrolabe fault (AST-C1) Mw = 7.1

The fault parameters used in modelling the composite Astrolabe fault are derived from Lamarche and Barnes (2005) with magnitude of Mw = 7.1. The fault length = 76.0 km; strike= 17.65^o; slip = 90.0^o, dip = 50.0^o, depth = 12.0 km and vertical displacement = 2.35 m. The Initial condition is illustrated in Figure 6.3.1-1. The model results show that the maximum tsunami elevations along the east coast of Waikato region are ranging from 0.5 to 1.5 m (Figure 6.3.1-2). The coastal area along Tairua experiences the highest maximum tsunami elevation of ~ 1.5 m, occurring along the Te Karo, Otara and Neaves Bays.

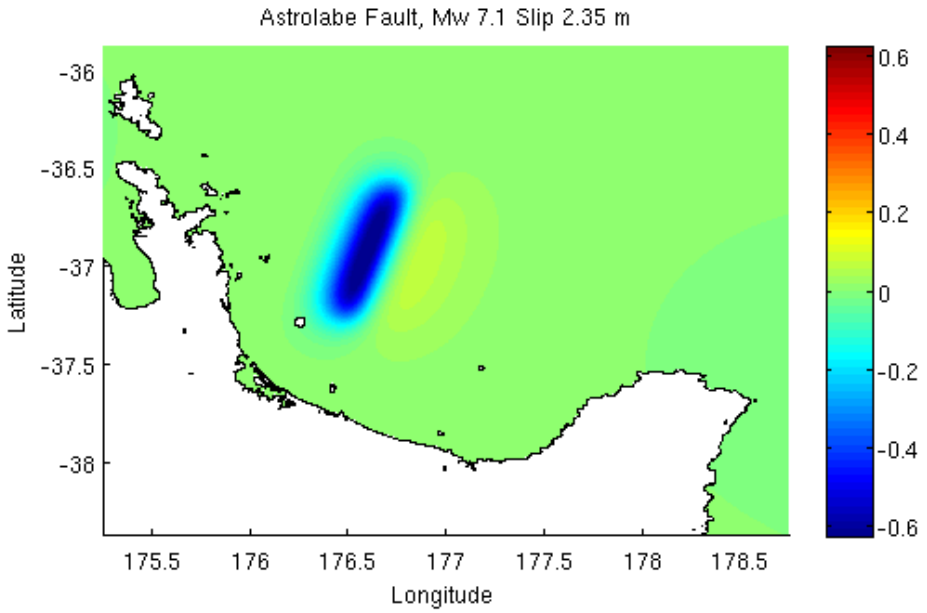

Figure 6.3.1-1 The initial condition of tsunami elevation above MSL at the source region. Scale bar unit is in metres.

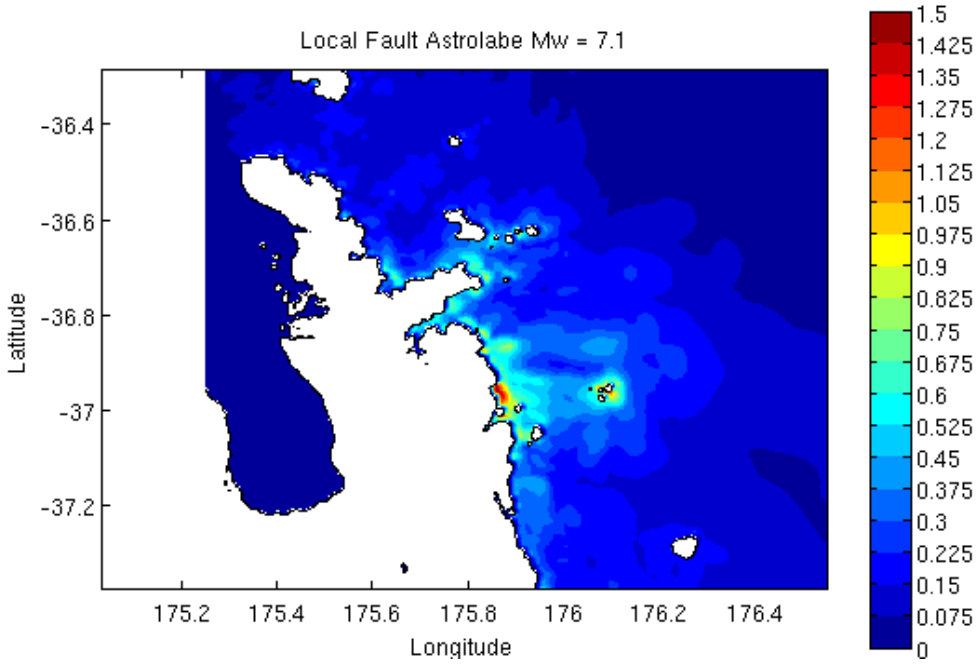

Figure 6.3.1-2 The maximum tsunami elevation above MSL along the east coast of Waikato Region varies from 0.5 m to 1.5 m. The concentration of maximum tsunami elevation occurs along Te karo, Otara and Neaves Bays north of Tairua. Scale bar unit is in metres.

6.3.2 A composite Volkner fault (VOLC-C1) Mw = 6.79

The fault parameters used in modelling the composite Volkner fault are derived from Lamarche and Barnes (2005) with magnitude Mw = 6.79. The fault length = 34.6 km; strike= 25.49°; slip = 90.0°, dip = 50°, depth = 8.0 km and vertical displacement = 1.39 m. The Initial condition is illustrated in Figure 6.3.2-1. The model results show that the maximum tsunami elevations along the east coast of Waikato region are ranging from 0.1 to 0.3 m (Figure 6.3.2-2) with the highest maximum tsunami elevation distribution occurring along the coast from Whitianga down to Whangamata.

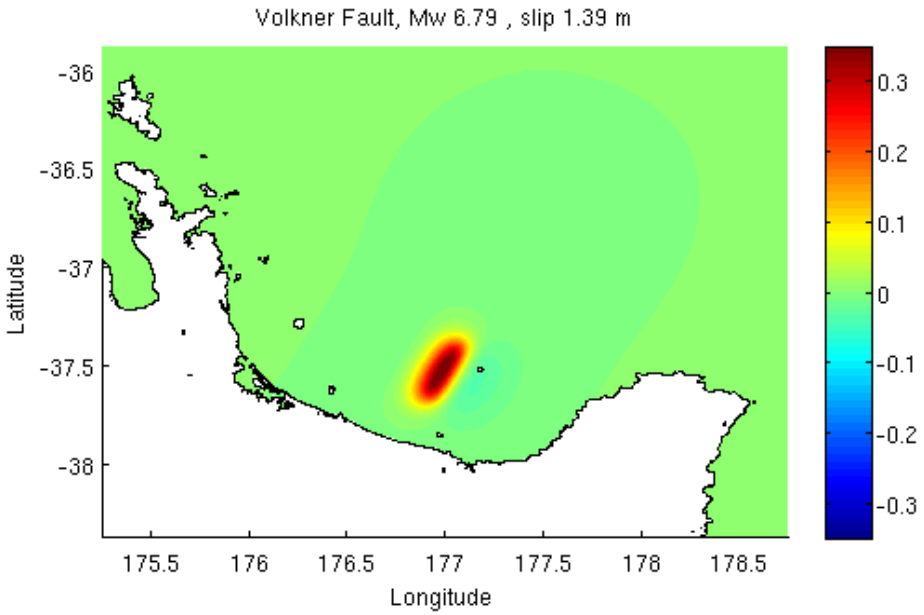

Figure 6.3.2-1 The initial condition of tsunami elevation above MSL at the source region. Scale bar unit is in metres.

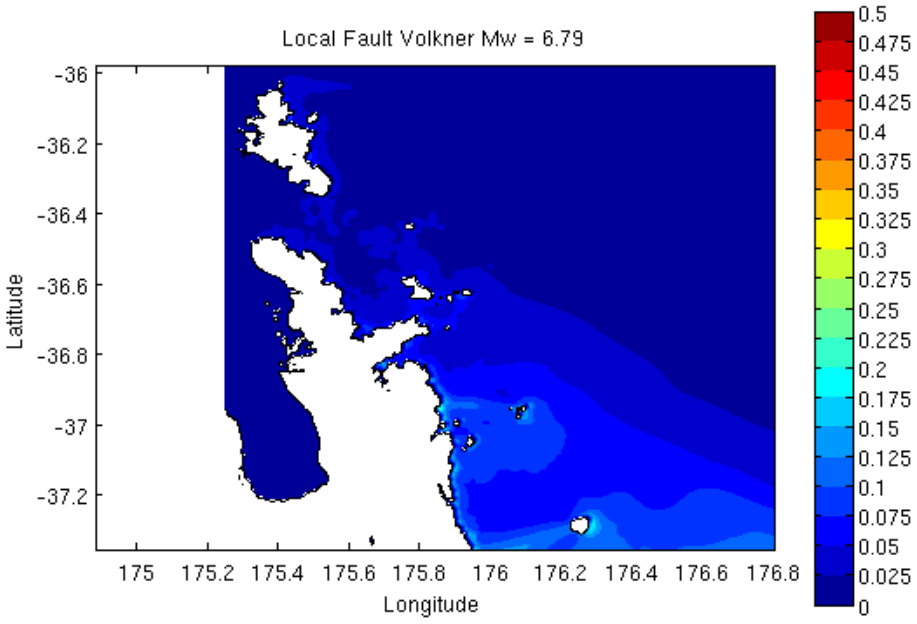

Figure 6.3.2-2 The maximum tsunami elevation above MSL along the east coast of Waikato Region varies from 0.1 m to 0.3 m. Scale bar unit is in metres.

6.3.3 A composite White Island fault (WIF-C1) Mw = 7.01

The fault parameters used in modelling the composite White Island fault are derived from Lamarche and Barnes (2005) with magnitude = 7.01. The fault length = 50.6 km; strike = 36.79°; slip = 90.0°, dip = 50.0°, depth = 8.0 km and vertical displacement = 2.03 m. The Initial condition is illustrated in Figure 6.3.3-1. The model results show that the maximum tsunami elevations along the east coast of Waikato region are ranging from 0.1 to 0.3 m (Figure 6.3.3-2) with the most affected areas being along the coast from Whitianga down to Whangamata.

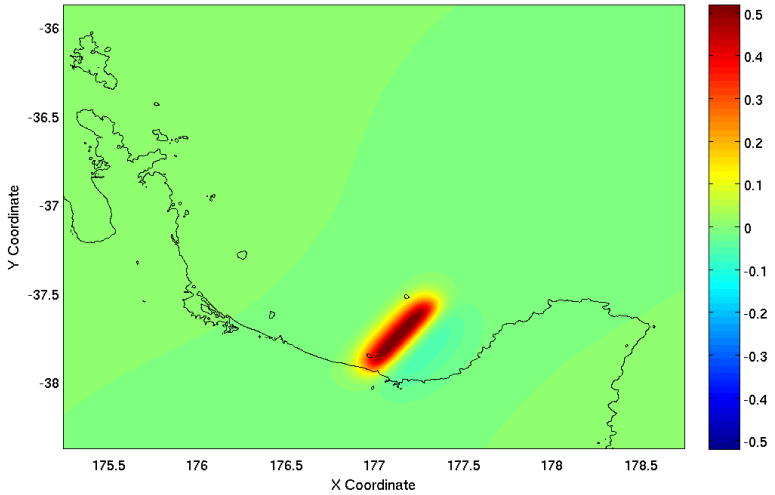

Figure 6.3.3-1 The initial condition of tsunami elevation above MSL at the source region. Scale bar unit is in metres.

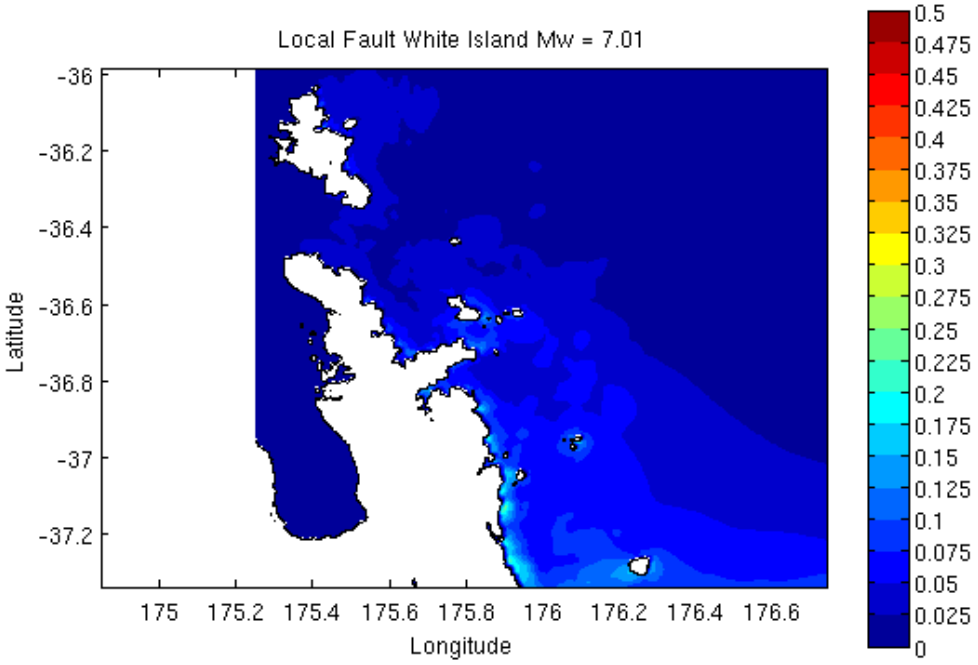

Figure 6.3.3-2 The maximum tsunami elevation above MSL along the east coast of Waikato Region varies from 0.1 m to 0.3 m. Scale bar unit is in metres.

7.0 CONCLUSIONS

- We present an overview of the previous and recent tsunami hazards research relevant to the eastern Coromandel Peninsula and east coast of Waikato region through:

  - assessing all relevant publications related to tsunami hazard assessment for Eastern Coromandel Peninsula;

  - clustering tsunami source definitions for the region from the Tonga-Kermadec source area; and

  - applying numerical modelling approaches to tsunami generation, propagation and inundation, incorporating source bathymetry and topography data;

  This work provides a consistent result on the potential tsunami impact to the region. These regions are highly susceptible to a tsunami generated from the Kermadec Trench. The source region extending from the East Cape Ridge to the northeast across the Rapuhia Scarp up to the central of Kermadec Trench (central and southern segment) provides a significant impact to the eastern Coromandel and along the east coast of Waikato region. The regional numerical modelling assessment for individual segment ruptures shows that the southern and central segments (Mw 8.5 to 8.9) provide a significant impact to the region with maximum tsunami elevation at the coast ranges from 3 to 5 m. The numerical modelling simulates the tsunami generated by a rupture of the entire Kermadec Trench and the possible extension to the Hikurangi Margin (Mw > 9.0). Maximum elevations in this scenario range from 8 m to 15 m above MSL, and 12 to 18 m (peak to trough) using an empirical formula of Abe (1995). Detailed inundation modelling

is needed to quantify the extent of inundation and the local effects that contribute in amplifying or reducing the tsunami height.

- We present the uncertainties associated with the Tonga-Kermadec source region in generating a tsunami through:
  - a discussion of the seismicity and slip partitioning of large shallow earthquakes;
  - a description of paleo-tsunami deposits;
  - a discussion of the role of sediment thickness on the subduction zone and related seismicity and tsunami genesis;

    These lines of evidence suggest that event scenarios involving the entire rupture of the Kermadec Trench (segment A, B and C of Power et al.2011; segments 2, 3 and 4 of this study; or southern, central and northern segment of previous studies of Goff et al. 2006, De Lange et al. 2008) in the logic tree are unlikely to ever occur as only 12% weighting was assigned to a magnitude frequency distribution that permits ruptures as large as Mw 9.4 to take place (Power et al. 2011). However, this scenario is taken into account (Power et al. 2011) as the possibility of rupture of the entire trench cannot be ruled out empirically (McCaffrey, 2007), and the 2004 Sumatra earthquake – Indian Ocean Tsunamis - involved a more than 1250 km length of fault ruptures with magnitude ~ Mw = 9.2 occurred at the place that was thought impossible to generate such a large earthquake (McCaffrey, 2008). Furthermore, recent work on paleo-tsunamis along the North Island New Zealand (Goff et al. 2010) provides evidence for continuous spread of tsunami deposits in ~AD1450's along the North Island commensurate with tsunami height distribution patterns from tsunamis generated by the scenario events that involve rupture of the entire Kermadec Trench.

- We define estimate potential return periods for tsunami generated from the Tonga-Kermadec region through:
  - a review of Tonga-Kermadec Trench seismicity based on published data and reports,
  - the application of McCaffrey (2008) methods to determine possible maximum earthquakes from the Tonga-Kermadec Trench,
  - computation of potential tsunami heights based on the methods of Abe (1995),

    These show that large events may take place within 600 to 800 years for even greater than Mw =9.0 with maximum tsunami wave height (peak to trough) up to 18 m, and up to 8 m (peak to trough) every ~ 400 years ($Mw \leq 9.0$).

- The numerical modelling from the local sources within the Bay of Plenty show that the maximum tsunami impact is produced by the Astrolabe composite fault with maximum tsunami elevation above MSL along the east coast of Waikato region ranges from 0.5 to 1.5 m. This fault had a typical return period for these faults vary from few hundred to 1000's of years (Lamarche and Barnes, 2005).

8.0 ACKNOWLEDGEMENTS

The author would like to thank Dr. Bill Fry of GNS Science and Dr. Vernon Pickett of Environment Waikato in carefully reviewing the manuscripts and provided valuable discussions and comments, and Penny Murray for her support and general assistances in producing the report.

9.0 REFERENCES

Abe, K. (1995). Estimate of Tsunami Runup heights from Earthquakes Magnitudes, in Y.Tsuchiya and N.Shuto (eds). Tsunami: Progress in Prediction, Disaster Prevention and Warning, Kluwer Academic Publishers, Dordrecht. Pages 21-35.

Bell, R.G., Goff, J., Downes, G., Berryman, K., Walters, R.A., Chague-Goff, C., Barnes, P. and Wright, I. (2004). Tsunami Hazards for the Bay of Plenty and Eastern Coromandel Peninsula: Stage 2. Environment Waikato Technical Report 2004/32. ISSN 1172-4010.

Billen, M.I., and Gurnis, M. (2005). Constraints on Subducting Plate Strength within the Kermadec Trench. Journal of Geophysical Research. Vol.110.B05407. pages 1-18. doi:10.1029/2004JB003308.

Billen, M.I., Grunis, M., and Simons, M. (2003). Multisclae dynamic of the Tonga-Kermadec Subduction Zone. Geophysical Journal International. Vol. 153. Pages 359-388.

Bonnardot, M.A., Regnier, M., Ruellan, R., Christova, C., and Tric, E. (2006). Seismicity and State of Stress within the Overriding plate of the Tonga-Kermadec Subduction Zone. Tectonics. Vol. 26. TC5017. Pages 1-15. doi: 10.1029/2006TC002044.

Christensen, D.H., and Ruff, L.J. (1988). Seismic Coupling and Outer Rise Earthquakes. Journal of Geophysical Research. Vol.93. No.B11. Pages 13,421-13,444.

Clift, P.D., MacLeod. C.J., Tappin, D.R., Wright., D.J., Bloomer, S.H. (1998). Tectonic Controls on Sedimentation and Diagenesis in the Tonga Trench and Forearc, Southwest Pacific. GSA Bulletin. Vol.110. No. 4. Pages 483-496.

Davy, B., and Collot, J.Y. (2000). The Raphuia Scarp (northern Hikurangi Plateau) – Its Nature and Subduction Effects on Kermadec Trench. Tectonotophysics. Vol. 328. Pages 269 – 295.

De Lange, W.P. and Healy, T.R.(2001). Tsunami Hazards for the Auckland Region and Hauraki Gulf, New Zealand. Natural Hazards, Vol24. Pages 267-284.

De Lange, W.P., Prasetya, G., Spiers, K.C., Moon, V.G. (2008). Utilising Paleotsunami Data for Hazard Assessment: Numerical Modelling to Identify Credible sources in Wallendorf, L., Ewing, L., Jones, C., and Jaffe, B. (eds). Solutions to Coastal Disaster 2008 – Tsunamis. American Society of Coastal Engineering. Pages 248-253.

De Lange, W.P., Prasetya, G. and Healy, T.R. (1999). Volcanoes and Tsunami hazards – Implications for New Zealand. TEPHRA October 1999. New Zealand.

Dmoska, R., Rice, J.R., Lovison, L.C., and Jossel, D. (1988). Strees Transfer and Seismic Phenomena in Coupled Subduction Zones During the Earthquake Cycle. Journal of Geophyiscal Research. Vol. 93. No.B7.Pages 7869-7884.

Fuller, W.C., Willett, S.D., Brandon, M.T.: 2006. Formation of forearc basins and their influence on subduction zone earthquakes, Geology. Vol.34. No.2. Pages 65-68

Garcia-Castellanos, D., Torne, M., and Fernadez, M. (2000). Slab Pull Effects from a Flexural Analysis of the Tonga and Kermadec Trenches (Pacific Plate). Geophysical Journal International. Vol.141. Pages 479-484.

Geist, E., and Parsons, T. (2006). Probabilistic Analysis of Tsunami Hazards. Natural Hazards. Vol. 37. Pages 277-314.

Goff, J., Pearce, S., Nichol, S.L., Chague-Goff, C., Horrocks, M., Strotz, L. (2010). Multi-proxy record of regionally source tsunamis, New Zealand. Geomorphology. Vol.118. Pages 369-382.

Goff, J., Walters, R., and Callaghan, F. (2006). Tsunami Source Study. Environment Waikato Technical Report 2006/49. ISSN: 1172-4005.

Goff, J.(2003). Joint Tsunami research Project; Stage 1.GeoEnvironmental Client Report: GEO2003/20028, prepared for Environment Bay of Plenty and Environment Waikato. 49 p.

Hilde, T.W.C. (1983). Sediment Subduction Versus Accretion Around the Pacific. Tectonophysics. Vol. 99. Pages 381-397.

Lamarche, G. and Barnes, P. (2005). Fault Characterisation and Earthquake Source Identification in the Offshore bay of Plenty. NIWA Client Report: WLG2005-51. 57 pp. 36 Figs.

Lewis, K.B., Collot, J.Y., and Lallemand, S.E. (1998). The Dammed Hikurangi Trough: a Channel-fed Trench Blocked by Subducting Seamounts and Their Wake Avalanches (New Zealand-France GeodesyNZ Project). Basin Research. Vol.10. Pages 441-468.

Lundgren, P.R., Okal, E.A., and Wiens, D.A. (1989). Rupture Characteristics of the 1982 Tonga and 1986 Kermadec Earthquakes. Journal of Geophysical Research. Vol. 94. No. B11. Pages 15,521-15,539.

McCaffrey, R. (2008). Global Frequency of Magnitude 9 Earthquakes. The Geological Society of America. Vol.36 .No.3. Pages 263-266

McCaffrey, R. (2007), The Next Great Earthquake, *Science* 23 March 2007 315: 1675-1676.

McFadgen, B.G. and Goff, J.R.(2007). Tsunamis in the New Zealand archaeological record. Sedimentary Geology. Vol.200. Pages 263-274.

Molnar, P., Freedman, D., and Shih, J.S.F. (1979). Lengths of intermediate and deep seismic zones and temperatures in down going slabs of lithosphere. Geophysical Journal of Royal Astronomy Society. Vo. 56. Pages 41-54.

Okal., E. and Romanowicz, B. (1994). On the Variation of b-values with Earthquake Size. Physics of the Earth and Planetary Interiors. Vol. 87. Pages 55-76.

Papazachos, B.C., Papadimitriou, E.E., Karakaisis, G.F., and Panagiotopoulos. (1997). Long-term Earthquake Prediction in the Circum-Pacific Convergent Belt. Pure and Applied Geophysics. Vol. 149. Pages 173-217.

Pelletier, B., and Louat, R. (1989). Seismotectonics and Present-Day Relative Plate Motions on the Tonga_-Lau and Kermadec-Havre Region. Tectonophysics. Vol.165. Pages 237 – 250.

Pachecho, J.F., Sykes, L., and Scholz, C. (1993). Nature of Seismic Coupling Along Simple Plate Boundaries of the Subduction Type. Journal of Geophysical Research. Vol. 98. No.B8. Pages 14,133-14,159.

Papadimitriou, E.E. (1994). Long-term Earthquake Prediction of Large Shallow Mainshocks along the Tonga-Kermadec-New Zealand seismic zone based on a Time- and Magnitude-Predictable model. Tectonophysics. Vol.235. Pages 347-350.

Power, W., Wallace, L.M., Wang, X., Reyners, M. (2011). Tsunami Hazards Posed to New Zealand by the Kermadec and Southern New Hebrides Subduction Margins: An Assessment Based on Plate Boundary Kinematics, Interseismic Coupling, and Historical Seismicity. Pure and Applied Geophysics. Doi:10.1007/s00024-011-0299-x.

Prasetya, G. (1998). Modelling of Volcanic Tsunamis. MSc Thesis. Department of Earth Sciences. University of Waikato.

Prasetya, G., De Lange, W.P. and Healy, T.R. (2000). Volcanic Tsunami Generation Mechanism Based on Krakatau event 1883 and Future Mitigation in Shuto N.(Ed). Regional report on Tsunami Research. Disaster Control Research Center – Tohoku University, Sendai. Japan.

Prasetya, G., De Lange, W.P., and Healy, T.R. (2008). Hydrodynamic Modelling of Tsunami Overwash of Whitianga Township and Harbour. Coastal Marine Group. The University of Waikato. Technical Report for Environment Waikato. 95 pages.

Ruff, L.J. (1989). Do Trench Sediment Affect Great Earthquake Occurrence in Subduction Zone. Pure and Applied Geophysics. Vol. 129. Pages 263-282.

Ruff, L.J., and Kanamori, H. (1983). Seismic Coupling and Uncoupling at Subduction Zone. Tectonophysics. Vol. 99. Pages 99 – 117.

Sandwell, D.T., and Smith, W.H. (1997). Marine Gravity Anomaly from GEOSAT and ERS 1Satellite Altimetry. Journal of Geophysical Research, Vol.102. No.B5. Pages 10,0390-10,054.

Scholz, C.H., and Small. C. (1997). The effect of Seamount Subduction on Seismic Coupling. Geology. Vol. 25. No.6. Pages 487 – 490.

Wallace, L.M. et al. (2009). Characterizing the Seismogenic Zone of a Major Plate Boundary Subduction Thrust: Hikurangi Margin, New Zealand. Geochemistry Geophysics and Geosystem – an electronic Journal of the Earth Sciences. Vol.10.No.10. Pages 1-32.doi:10/1029/2009GC002610.ISSN.1525-2027.

Wallace, L.M., Beavan, J., McCaffrey, R., Darby, D. (2004). Subduction Zone Coupling and Tectonic Block Rotations in the North Island, New Zealand. Journal of Geophysical Research. Vol.109. No. B12406. doi:10.1029/2004JB003241. Pages 1-21.

Wallace, M.L., Ellis, S. and Mann, P. (2009). Collisional Model for Rapid Fore-arc Block Rotations, ARC Curvature, and Episodic Back-arc Rifting in Subduction Settings. Geochemistry Geophysics and Geosystem – an electronic Journal of the Earth Sciences. Vol.10.No.5. Pages 1-50.doi:10/1029/2008GC002220.ISSN.1525-2027.

Walters, R.A., Goff, J., and Wang, K. (2006). Tsunamigenic Sources in The Bay of Plenty, New Zealand. Science of Tsunami Hazards. Vol.24. No.5. Pages 339 -357.

Watts. A.B., Koopers. A.A.P., and Robinson, D.P. (2010). Seamount Subduction and Earthquakes. Oceanography. Vol.23.No.1. Pages 166 -173.

ITDB/PAC. (2004). Integrated Tsunami Database for the Pacific. Version 5.11 of July 2004. CD-ROM Tsunami Laboratory. ICMMG, SD RAS. Novosibirks, Russia.

Wang, X. (2010). COMCOT ver.1.7 User's Manual. GNS Science. New Zealand.

APPENDIX 1 — MAGNITUDE – RETURN PERIOD AND TSUNAMI HEIGHT ESTIMATION

Table.5.2.1 The computation results using McCaffrey (2008) and Abe (1985) methods without fault width correction factors.

No	FAULT	Length	SLIP(Uav)	Zmax	dip angle	Mo	MwMax	Con. Rate		Return period		+/-	R	H_Abe
		(km)	(m)	(m)	(degree)	(dyne/cm2)	(Nm)	(mm/year)		(years)		(years)	(km)	(m)
								min	max	min	max			
1	**Segment1**	224	5.60	20000	16	2.73E+21	**8.22**	40	55	102	140	16	-	**0**
2	**Segment2**	273	6.83	20000	16	4.06E+21	**8.34**	40	55	124	171	16	371	**2.93**
3	**Segment3**	447	11.18	20000	16	1.09E+22	**8.62**	40	55	203	279	16	566	**3.71**
4	**Segment4**	517	12.93	20000	16	1.45E+22	**8.71**	55	60	215	235	16	932	**2.73**
5	**Segment5**	323	8.08	20000	16	5.68E+21	**8.43**	55	60	135	147	16	1320	**1.03**
6	**Combined 1,2**	497	12.43	20000	16	1.34E+22	**8.68**	40	55	226	311	16	371	**6.51**
8	**Combined 2,3**	720	18.00	20000	16	2.82E+22	**8.90**	40	55	327	450	16	371	**10.67**
9	**Combined 3,4**	964	24.10	20000	16	5.06E+22	**9.07**	40	55	438	603	16	566	**10.32**
10	**Combined 4,5**	840	21.00	20000	16	3.84E+22	**8.99**	40	55	382	525	16	932	**5.22**
11	**Combined 1,2,3**	944	23.60	20000	16	4.85E+22	**9.05**	40	55	429	590	16	492	**11.55**
12	**Combined 2,3,4**	1237	30.93	20000	16	8.33E+22	**9.21**	50	60	515	619	16	662	**12.31**
13	**Combined 3,4,5**	1287	32.18	20000	16	9.01E+22	**9.23**	55	60	536	585	16	702	**12.24**
14	**Combined 1,2,3,4**	1461	36.53	20000	16	1.16E+23	**9.31**	50	60	609	731	16	562	**18.10**
15	**Combined 2,3,4,5**	1560	39.00	20000	16	1.32E+23	**9.35**	55	60	650	709	16	702	**15.82**
16	**Combined 1,2,3,4,5**	1784	44.60	20000	16	1.73E+23	**9.42**	50	50	892	892	16	702	**18.91**

Remarks:

Con. Rate: Convergence rate; Mo, MwMax: moment magnitude of the earthquake, R = a distance from the center of segment to Eastern Coromandel Peninsula coast line; H_Abe: the tsunami height at the coast.

Table.5.2.2 The computation results using McCaffrey (2008) and Abe (1985) methods with maximum of 0.67 fault width correction factors.

No	FAULT	Length	SLIP(Uav)	Zmax	dip angle	Mo	MwMax	Con. Rate		Return period		+/-	R	H_Abe
		(km)	(m)	(m)	(degree)	(dyne/cm2)	(Nm)	(mm/year)		(years)		(years)	(km)	(m)
								min	max	min	max			
1	**Segment1**	224	3.73	20000	16	1.82E+21	**8.10**	40	55	50.91	70.00	15.59	-	**0.00**
2	**Segment2**	273	4.55	20000	16	2.7E+21	**8.22**	40	55	62.04	85.30	15.59	371	**2.24**
3	**Segment3**	447	7.45	20000	16	7.25E+21	**8.50**	40	55	95.27	131.00	15.59	566	**2.83**
4	**Segment4**	517	8.62	20000	16	9.7E+21	**8.59**	55	60	107.75	117.55	15.59	932	**2.08**
5	**Segment5**	323	5.38	20000	16	3.79E+21	**8.32**	55	60	67.33	73.45	15.59	1320	**0.79**
6	**Combined 1,2**	497	8.28	20000	16	8.96E+21	**8.57**	40	55	113.00	155.38	15.59	371	**4.97**
8	**Combined 2,3**	720	12.00	20000	16	1.88E+22	**8.78**	40	55	163.64	225.00	15.59	371	**8.15**
9	**Combined 3,4**	964	16.07	20000	16	3.37E+22	**8.95**	40	55	219.09	301.25	15.59	566	**7.88**
10	**Combined 4,5**	840	14.00	20000	16	2.56E+22	**8.87**	40	55	190.91	262.5	15.59	932	**3.98**
11	**Combined 1,2,3**	944	15.73	20000	16	3.23E+22	**8.94**	40	55	214.55	295.00	15.59	492	**8.81**
12	**Combined 2,3,4**	1237	20.62	20000	16	5.55E+22	**9.09**	50	60	257.75	309.30	15.59	662	**9.39**
13	**Combined 3,4,5**	1287	21.45	20000	16	6.01E+22	**9.12**	55	60	268.17	292.55	15.59	702	**9.34**
14	**Combined 1,2,3,4**	1461	24.35	20000	16	7.74E+22	**9.19**	50	60	304.42	365.30	15.59	562	**13.81**
15	**Combined 2,3,4,5**	1560	26.00	20000	16	8.83E+22	**9.23**	55	60	308.33	336.36	15.59	702	**12.07**
16	**Combined 1,2,3,4,5**	1784	29.73	20000	16	1.15E+23	**9.31**	50	50	446.00	446.00	15.59	702	**14.43**

Remarks:

Con. Rate: Convergence rate; Mo, MwMax: moment magnitude of the earthquake, R = a distance from the center of segment to Eastern Coromandel Peninsula coast line; H_Abe: the tsunami height at the coast. Rigidity = 3.10^{10}.